universität wien

DIPLOMARBEIT

Titel der Diplomarbeit

„Functional characterisation of the δ-subunit of the epithelial sodium channel (ENaC) in human bronchiolar and bronchial epithelial cells“

Verfasserin

Svenja Sladek

angestrebter akademischer Grad

Magistra der Pharmazie (Mag.pharm.)

Wien, November 2012

Studienkennzahl lt. Studienblatt:	A 449
Studienrichtung lt. Studienblatt:	Diplomstudiengang Pharmazie
Betreuerin / Betreuer:	Ao. Univ.-Prof. Mag. Dr. Franz Gabor

DANKSAGUNG

Besonders bedanken möchte ich mich bei Dr. Carsten Ehrhardt vom Trinity College Dublin für die kompetente Betreuung und das angenehme Arbeitsklima. Ich habe seinen Optimismus und Enthusiasmus stets geschätzt.

An dieser Stelle gilt mein Dank auch Ao. Univ-Prof. Mag. Dr. Franz Gabor, durch dessen Hilfe ich meine Diplomarbeit an der School of Pharmacy des Trinity College Dublin machen konnte.

Großer Dank gebührt meiner Betreuerin Elena Schwagerus für ihre Unterstützung, Geduld und die gute Zusammenarbeit, sowohl während des praktischen als auch während des schriftlichen Teils meiner Diplomarbeit.

Des Weiteren möchte ich mich bei Yamil Robles bedanken, der mir mit viel Geduld das Patch-clampen näher gebracht hat.

Ich möchte mich bei allen, besonders aber bei Johanna Salomon bedanken, die mir während meiner Zeit in Irland mit Rat und Tat zur Seite standen und dieses halbe Jahr unvergesslich gemacht haben.

Ganz herzlich danke ich auch allen Freunden, die mich während meines Studiums unterstützt und immer wieder motiviert haben.

Mein größter Dank gilt abschließend meinen Eltern, für die sowohl finanzielle als auch moralische Unterstützung und ihr Verständnis während meiner gesamten Ausbildung.

TABLE OF CONTENTS

LIST OF ABBREVIATIONS

ATI	Alveolar epithelial type I
ATII	Alveolar epithelial type II
ATCC	American Type Culture Collection
BSA	Bovine serum albumin
CFTR	Cystic fibrosis transmembrane conductance regulator
DAR	Diego Alvarez de la Rosa
DENaC	δ-ENaC over-expressing cells
DEX	Dexamethasone
DMSO	Dimethylsulfoxide
EB	Evans blue
EC_{50}	Half maximal effective concentration
ECACC	European Collection of Animal Cell Cultures
EGTA	Ethylene glycole tetraacetic acid
EMEM	Eagle's minimum essential medium
ENaC	Epithelial sodium channel
α	Alpha subunit
β	Beta subunit
γ	Gamma subunit
δ	Delta subunit
FBS	Foetal bovine serum
G418	Geneticin
HEPES	4-(2-hydroxyethyl)-1-piperazineethanesulfonic acid
HRP	Horseradish peroxidase

HSC	Highly Na^+-selective cation
IC_{50}	Half maximal inhibitory concentration
IFM	Immunofluorescence microscopy
I_{sc}	Short-circuit current
$K_{0.5}$	Inhibition constant
KRB	Krebs-Ringer-Buffer
LB	Luria Bertani
LCC	Liquid-covered culture
NSC	Non-selective cation
PBS	Phosphate-buffered saline
rpm	Revolutions per minute
SC	Santa Cruz Biotechnology
SDS-PAGE	Sodium dodecyl sulphate polyacrylamide gel electrophoresis
shCTRL	Mock-transfected cells
shDENaC	δ-ENaC knockdown transfectants
shRNA	Small hairpin RNA
siRNA	Small interfering RNA
TEER	Transepithelial electrical resistance
TEMED	N, N, N‘, N‘-tetramethylethylenediamine
Tris	Tris(hydroxymethyl)aminomethane
TRPV1	Transient receptor potential vanilloid subfamily 1
TTB	Towbing transfer buffer
wt	Wild-type

ABSTRACT – ENGLISH

The epithelial sodium channel (ENaC), consisting of various combinations of the four homologous subunits α, β, γ and δ, mediates the sodium transport across epithelial tissues. Delta-ENaC subunit mRNA and protein are present in the human lung tissue, raising the question about the physiological role of δ-ENaC in the lung. Therefore, we used a number of xenobiotics that have been suggested to be selective δ-ENaC modulators. The sodium-dependence of the alleged activators and inhibitors was confirmed by Ussing chamber experiments in sodium-free buffer. As the pharmacophores displayed different effects than published in previous papers, we further assessed the δ-ENaC specificity of the substances by knock-down as well as over-expression studies of δ-ENaC protein. In summary, our observations revealed that the compounds' effects in the organotypic cell models most likely originated from modulation of other, yet unknown, targets. The identification of more specific δ-ENaC modulators is required in order to further study the functional expression as well as the physiological role of δ-ENaC in the lung epithelium and other tissues.

ABSTRACT – DEUTSCH

Der epitheliale Natriumkanal (ENaC), der aus verschiedenen Kombinationen der homologen Untereinheiten α, β, γ und δ besteht, ist für den epithelialen Natriumtransport verantwortlich. Sowohl δ-ENaC mRNA als auch das Protein wurden in der menschlichen Lunge nachgewiesen; um die Expression und physiologische Rolle von δ-ENaC im epithelialen Lungengewebe näher zu untersuchen, haben wir eine Reihe von Pharmakophoren verwendet, die als δ-ENaC Modulatoren beschrieben worden sind. Zuerst wurde die Natriumabhängigkeit der Agonisten und Antagonisten anhand von Ussingkammerexperimenten bestätigt. Da die ENaC-Modulatoren andere als die zuvor publizierten Ergebnisse lieferten, haben wir mit Hilfe von δ-ENaC Herabregulierung und Überexpression versucht die Spezifität der Modulatoren zu untersuchen. Alles in allem haben unsere Studien gezeigt, dass die durch die Substanzen hervorgerufenen Effekte wahrscheinlich durch die Interaktion mit anderen Zielstrukturen hervorgerufen werden. Aus diesem Grund ist es nötig weitere und spezifischere δ-ENaC Modulatoren zu identifizieren, um sowohl Expression als auch physiologische Funktion von δ-ENaC genauer untersuchen zu können.

1 INTRODUCTION AND BACKGROUND

1.1 The epithelial sodium channel

The epithelial sodium channel (ENaC) is an amiloride-sensitive, non-voltage gated ion channel, widely distributed throughout epithelial as well as non-epithelial tissues. It belongs to the ENaC/degenerin superfamily of ion channels, members of which display a remarkable functional diversity including Na^+ absorption, acid-sensing, peptide-gating, acidosis-evoked nociception and mechanotransduction. There have been 5 subunits (α, β, γ, δ, ε) cloned so far that are able to assemble in different combinations [1, 2].

1.1.1 The canonical ENaC (αβγ)

The heteromeric channel, mostly found in epithelial tissue, consists of the three homologous subunits α, β and γ. Albeit sharing 34-37% of their amino acid sequence, each subunit is encoded by a different gene [3, 4, 5].

Another common feature is the membrane topology, which is shown in **Figure 1**. ENaC subunits have two hydrophobic transmembrane regions (M1, M2) that are separated by an extracellular, hydrophilic loop with several glycosylation sites and a short intracellular amino as well as a carboxy terminus. The pre-M2 segment is thought to be the pore-forming part in all ENaC subunits [2, 5, 6, 7].

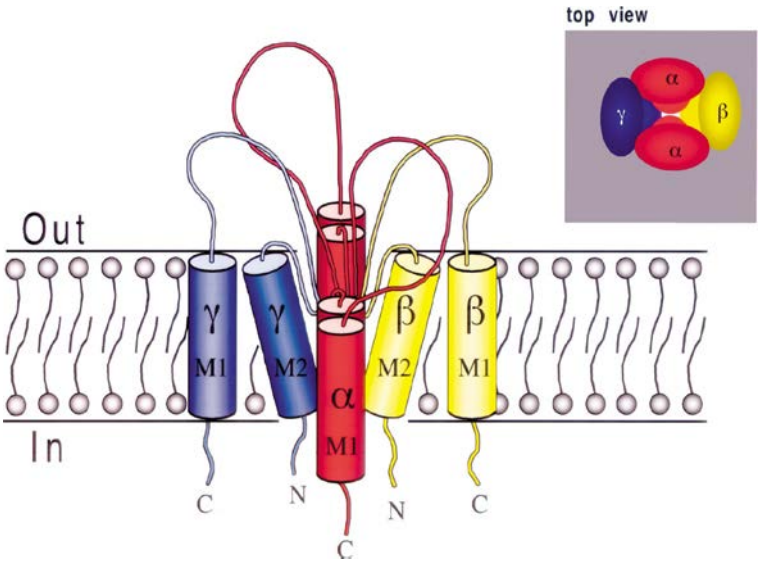

Figure 1

ENaC structure and membrane topology. The canonical ENaC is composed of 3 homologous subunits: α, β, and γ, in a tetrameric configuration. Subunits have similar membrane topology, characterised by two transmembrane domains (M1 and M2), an extracellular loop and cytoplasmic amino and carboxyl termini [8].

Canessa *et al.* demonstrated that β- or γ-ENaC are not able to induce amiloride-sensitive Na^+ currents on their own, whereas the expression of α-ENaC alone generated Na^+ currents [4]. However, larger currents resulted from the combination of αβ- or αγ-ENaC. For maximal activity, the assembly of all three ENaC subunits is required. This has been proposed to be a tetrameric 2αβγ- or a nonameric 3α3β3γ-construct [9, 10].

The canonical ENaC (αβγ) is expressed in the cortical and collecting tubules of the kidney, distal colon, ducts of secretory glands and in distal and proximal airways. In these epithelia, it is localised to the apical cell membranes and provides - together with the basolateral Na^+/K^+-ATPase - a pathway for

transepithelial sodium transport. Therefore, ENaC plays a crucial role in controlling the body's Na^+ homeostasis and, hence, extracellular volume as well as blood pressure [1, 2, 11].

In the respiratory tract, αβγ-ENaC is expressed from the nasal to the alveolar epithelium and plays a critical role at birth, when the lung changes from a liquid- to an air-filled organ [1, 12]. Hummler *et al*. demonstrated the importance of α-ENaC in particular, since α-ENaC knockout mice died soon after birth from respiratory failure, caused by deficient liquid clearance from the lung [13]. Additionally, β- and γ-ENaC knockout mice displayed reduced, albeit sufficient, alveolar fluid clearance and died from hyperkalaemia due to abnormal K^+-reabsorption in the kidneys [14, 15].

1.1.2 The δ-ENaC subunit

In addition to the above mentioned α-, β-, γ-ENaC subunits, there is a forth one, δ-ENaC, which has been cloned from the human kidney. In contrast to the canonical ENaC, this subunit is also widely distributed throughout non-epithelial tissues. The highest expression of δ-ENaC mRNA was found in testis, ovary, pancreas and brain; whereas, smaller amounts were detected for example in the kidney and lung [16]. Yamamura *et al.* confirmed the presence of δ-ENaC in heart, liver, pancreas, in the different parts of the brain, oesophagus, skin, skeletal muscle and in adult as well as foetal human kidney [17, 18, 19]. Furthermore, δ-ENaC has been described in cultured human epithelial cell lines of the pancreas (CFPAC), the colon (Caco-2) and the lung (H441 and A549) on mRNA as well as on protein levels (H441 and A549 cells) [20]. Finally, a recent

study by Bangel-Ruland *et al.* reported the presence of δ-ENaC in human nasal epithelium on the mRNA, protein and functional levels [21].

Regarding its amino acid sequence, δ-ENaC is closer related to α-ENaC (37% homology) rather than to β- and γ-subunits (27% and 29%, respectively). The transmembrane topology is identical for all four subunits [16].

Expressed in *X. laevis* oocytes on its own, δ-ENaC, similar to α-ENaC, produced a Na^+ current, which is around 50 times lower than the current induced by δβγ-ENaC. However, unlike in the case of the α-ENaC subunit, no currents were generated when δ-ENaC was co-expressed with only α-, β- or γ-ENaC.

Besides the tissue distribution, there are also differences between α- and δ-ENaC in the pharmacology and ion selectivity. In order to block δ-ENaC, significantly higher concentrations of amiloride and benzamil are needed. Also, δ-ENaC displayed a higher permeability for Na^+ than it does for Li^+, while both subunits were impermeable for K^+ [16].

So far, little is known about the physiological role of δ-ENaC. Since it is activated by protons, Yamamura and colleagues have suggested that δ-subunit may act as a pH sensor in the human brain and oesophagus [17, 18, 22]. In inflamed and hypoxic tissue, δ-ENaC could be a part of a mechanism integrating external ischemic signals [23, 24]. Recent studies suggested that δ-ENaC may also act as a pH sensor in the lung and respond to noxious acidic aspiration [25].

1.2 The electrophysiology of the epithelial lung tissue

As described previously, epithelial sodium channels play an important role in alveolar fluid clearance at birth and in maintaining the lung fluid balance thereafter [13, 14, 15].

On the one hand, epithelial lung tissue constitutes a barrier between an air-filled compartment and a vascular compartment. On the other hand, it facilitates the alveolar exchange of O_2 and CO_2. The alveolar lining layer, composed of surfactant and an aqueous subphase, is crucial to this process [26]. The balance between the passive fluid transport from the vascular compartment into the airways due to hydrostatic pressure and the liquid reabsorption, caused by the transepithelial Na^+ uptake, creates the moist environment of the lung [27, 28].

Alveolar type I (ATI) and alveolar type II (ATII) epithelial cells, which cover approximately 99% of the internal surface of the lung, are the cellular sites of the major part of the alveolar ion and fluid absorption in the adult lung (**Figure 2**). ATI cells are large, squamous cells with very thin cytoplasmic extensions that cover about 98% of the internal lung surface [29]. They are involved in alveolar homoeostasis, lung development and remodelling, host defence, tumour-growth suppression, etc. [30, 31]. ATII cells are smaller, cuboidal cells that synthesise, secrete and re-uptake pulmonary surfactant [32]. As progenitor cells, they are also important in the process of repairing injured alveolar epithelium [33].

Prenatally, Cl^- secretion is the main alveolar ion transport process that accounts for the lung being filled with liquid [34]. At birth, the pattern of alveolar fluid

secretion changes to that of fluid absorption, which is due to Na^+ absorption becoming the predominant process [35].

Both ATI and ATII cells express functional ENaC and are involved in sodium absorption [36]. Sodium is absorbed via ENaC on the apical side of the epithelium and then actively transported across the basolateral membrane into the lung interstitium by the Na^+/K^+-ATPase. Thus, an osmotic gradient is generated that forces Cl^- and water to follow via CFTR (cystic fibrosis transmembrane conductance regulator) channels and aquaporins, respectively. This process can be inhibited either by amiloride (ENaC-inhibitor) or ouabain (Na^+/K^+-ATPase-inhibitor) [29].

In patch-clamp studies carried out in ATII cells, two distinct types of Na^+ channels were detected: *(i)* the highly Na^+-selective cation (HSC) channels, consisting of α-, β- and γ-subunits, with a unit conductance of 4-6 pS and a Na^+/K^+-selectivity over 40 [37, 38] and *(ii)* non-selective cation (NSC) channels, composed of the α-subunit alone and displaying a unit conductance of 19-24 pS and a Na^+/K^+ selectivity of approximately 1 [27, 38, 39, 40].

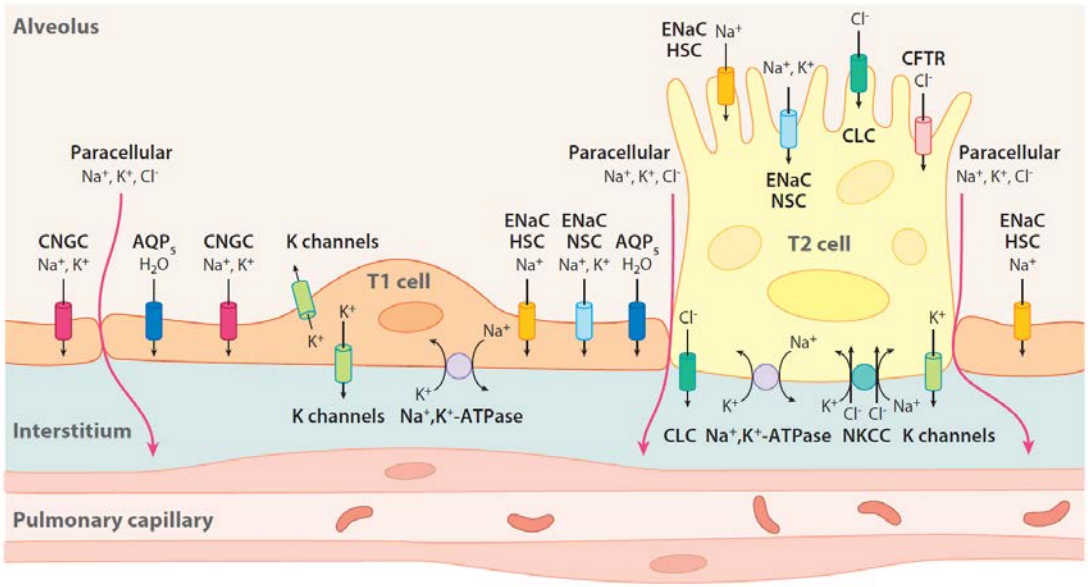

Figure 2

Schematic diagram of alveolar epithelial ion and fluid transport. Na^+ is absorbed from the apical surfaces of both ATI and ATII cells via ENaC (HSC and NSC channels). Electroneutrality is conserved by Cl^- movement through CFTR or CLC channels in ATII cells and/or paracellular influx, through tight-junctions. Na^+ is transported from the basal surface of both cell types into the interstitial space by Na^+/K^+-ATPase. If net ion transport occurs from the apical surface to the interstitium, an osmotic gradient is created. This gradient in turn directs water transport in the same direction, either through aquaporins or by diffusion [41].

However, additional amiloride-sensitive cationic channels with various physiological properties have also been reported, which contribute to the diversity of pulmonary channel expression and function [36, 42].

Junor *et al.* discovered that, although amiloride completely abolished basal liquid resorption in neonatal sheep, the process became less sensitive to amiloride in adult sheep [43]. Furthermore, studies in adult rats revealed that only 30% of the baseline lung fluid absorption was blocked by silencing the α-ENaC expression using RNAi and the remaining fluid absorption was not inhibited by amiloride [44].

These observations indicate that the canonical ENaC becomes less important in the lung fluid absorption as the lung changes from neonatal to adult life [29].

The recent evidence for presence of δ-ENaC in human respiratory epithelial cells on mRNA and protein levels, taken together with the observation that the major part of the baseline lung fluid absorption is not mediated by α-ENaC and displays smaller sensitivity to amiloride in the adult lung, raised the question, whether δ-ENaC contributes to the variety of sodium conductances and, thus, to the fluid clearance in the lung.

1.3 Pharmacological modulators of ENaC function

Pharmacological tools available to distinguish between α- and δ-ENaC mediated currents are limited to date and are presented below.

Non-selective pore blocker: amiloride (**Figure 3**)

Amiloride is a potassium-sparing diuretic that is mainly used to treat hypertension and congestive heart failure.

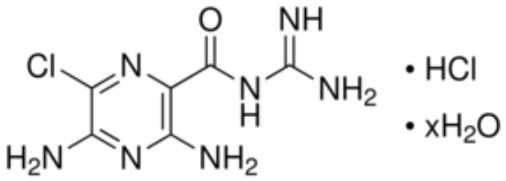

Figure 3

3,5-diamino-6-chloro-*N*-(diaminomethylene)pyrazine-2-carboxamide

It blocks the aldosterone-sensitive sodium absorption by reducing the mean open time of the ENaC channel in the kidney and decreases the potassium excretion in the distal nephron [45].

Both, δ-ENaC as well as α-ENaC, channels are inhibited by amiloride; however, δβγ-ENaC is 30-fold less sensitive ($K_{0.5}$ = 2.6 µM) to amiloride than αβγ-ENaC channels ($K_{0.5}$ = 80 nM), making it possible to distinguish between α-ENaC and δ-ENaC induced currents [16].

Selective antagonist: Evans blue (**Figure 4**)

Evans blue is a non-toxic azo-dye that is used to study blood vessel and cellular membrane permeability as well as to measure the blood volume due to its high affinity to albumin [46].

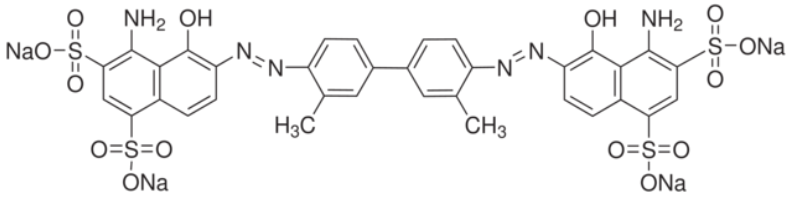

Figure 4

Tetrasodium (6*E*,6'*E*)-6,6-[(3,3'-dimethylbiphenyl-4,4'-diyl)di(1*E*)hydrazin-2-yl-1-ylidene]bis(4-amino-5-oxo-5,6-dihydronaphthalene-1,3-disulfonate)

Evans blue inhibited the inward currents generated by δβγ-ENaC, heterologously expressed in *Xenopus laevis* oocytes in a concentration-dependent manner with an IC_{50} of 143 µM. Additionally, the homomeric δ-ENaC channel was also blocked by Evans blue, however, not the αβγ-ENaC. The latter even showed a slight increase in activity in response to Evans blue [47].

Selective agonists: capsazepine and icilin **(Figure 5 and Figure 6)**

Capsazepine was developed as a synthetic analogue of the sensory neuron excitotoxin, capsaicin. It is a competitive antagonist for the transient receptor potential vanilloid subfamily 1 (TRPV1) and, therefore, a competitive antagonist of capsaicin as well as the more potent resiniferatoxin [48, 49, 50].

At micromolar concentrations, it also blocks voltage-dependent calcium and potassium channels [51, 52] as well as nicotinic acetylcholine receptors [53].

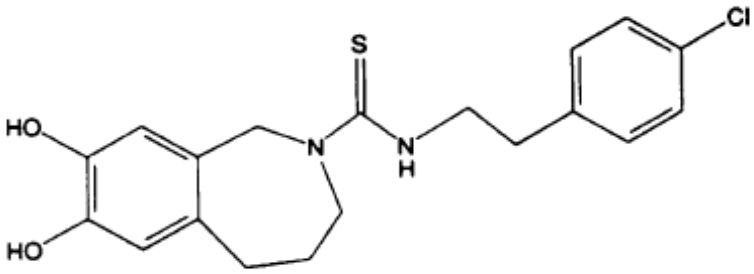

Figure 5

(2-[2-(4-chlorphenyl)ethylamino-thiocarbonyl]-7,8-dihydroxy-2,3,4,5-tetrahydro-lH-2 benzazepine)

More recently, it was reported that capsazepine also potentiates the activity of the human δβγ-ENaC in a concentration-dependent manner with an EC_{50} of 8 μM. The effect of capsazepine is reversible and amiloride-sensitive [54].

Icilin is a super-cooling agent, acting as an agonist for the transient receptor potential melastatin subfamily 8 (the cold-receptor) and ankyrin-like subfamily 1 [55, 56, 57].

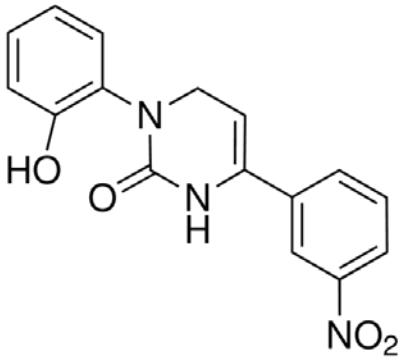

Figure 6

1-(2-Hydroxyphenyl)-4-(3-nitrophenyl)-1,2,3,6-tetrahydropyrimidin-2-one

Yamamura and co-workers have shown that icilin activates the human δβγ-ENaC in a concentration-dependent manner with an EC_{50} of 33 µM. The application of icilin increased the inward currents in δβγ-ENaC expressing *X. laevis* oocytes significantly. This effect was abolished by amiloride or by the removal of external Na^+ [58].

All in all, capsazepine and icilin acted as activators for the heteromeric human δβγ-ENaC as well as for the homomeric δ-ENaC in *X. laevis* oocytes, but caused a slight decrease in the inward currents mediated by αβγ-ENaC.

This led to the conclusion that both compounds were selective δ-ENaC activators and may also be used to elucidate the functional role of the channel in more complex cell and tissue models [54, 58].

1.4 Aim

The objective of this project was to investigate the expression, cellular localisation and the function of δ-ENaC in human respiratory epithelial cells *in*

vitro. In particular, we aimed to test the specificity of the alleged δ-ENaC modulators in H441 and Calu-3 cells. To this end, δ-ENaC downregulation (in H441 and Calu-3 cells) as well as δ-ENaC overexpression (in H441 cells only) were performed, and the effects thereof were studied on protein as well as on the functional levels. Furthermore, the effects of the reported δ-ENaC modulators in H441 were evaluated in regards to their sodium dependence.

2 MATERIALS AND METHODS

2.1 Materials

Rabbit anti-δ-ENaC polyclonal antibodies, used in this work, were purchased from Santa Cruz Biotechnology (sc-21015, Heidelberg, Germany) or kindly provided by Dr. Diego Alvarez de la Rosa (Universidad de La Laguna, La Laguna, Spain). All other primary antibodies were obtained from Millipore (mouse anti-Na^+/K^+-ATPase α-1 clone C464.6 monoclonal antibody, Carrigtwohill, Ireland) or Sigma-Aldrich (mouse anti-β-actin monoclonal antibody, clone AC-15, A1978, Dublin, Ireland). Anti-mouse and anti-rabbit IgG horseradish peroxidase (HRP) conjugates (Promega, Medical Supply Company, Dublin, Ireland) were used as secondary antibodies. Cell culture media and all other reagents were obtained from Sigma-Aldrich.

2.2 Cell culture

Cells were grown on 6-well and 24-well plates for Western blot experiments and on Petri dishes (diameter 35 mm) for patch-clamp studies. For all experiments requiring polarised cell monolayers (i.e., Ussing chamber measurements, biotinylation assays), cells were seeded on Transwell Clear filter inserts (3460, VWR, Dublin, Ireland) and cultured under liquid-covered culture conditions (LCC). The transepithelial electrical resistance (TEER) of filter-grown cell monolayers was measured using a Millicell ERS Volt-Ohm Meter with STX-2 chopstick electrodes (Millipore) and corrected for the background value contributed by the filter inserts and medium. The measurements were conducted every other day

before changing the medium. All cell lines were cultured in humidified atmosphere of 95% air and 5% CO_2 at 37°C.

2.2.1 Calu-3 cell line

Calu-3 cells (American Type Culture Collection, ATCC HTB-55), human bronchial epithelial cells derived from an adenocarcinoma of the lung (by Fogh and Trempe, 1975), were obtained from the European Collection of Animal Cell Cultures (ECACC, Salisbury, UK).

Calu-3 cells were grown in Eagle's minimum essential medium (EMEM), supplemented with 10% foetal bovine serum (FBS), 100 U/ml penicillin, 100 µM/ml streptomycin, 1 mM sodium pyruvate, 0.1 mM non-essential amino acids and 15 mM glucose. Cells were seeded at a density of 100,000 cells/cm^2 on Transwell Clear inserts. A seeding density of 75,000 cells/cm^2 was used for seeding on other cell culture plastics.

2.2.2 H441 cell line

The bronchiolar epithelial H441 cell line (American Type Culture Collection, ATCC HTB-174), purchased from LGC standards (Teddington, UK) was derived from a papillary adenocarcinoma of the lung (by Gazdar et al., 1982).

H441 cells were cultured in RPMI-1640 Medium (Invitrogen, Biosciences, Dun Laoghaire, Ireland), supplemented with 10% FBS, 100 U/ml penicillin, 100 µM/ml streptomycin, 1 mM sodium pyruvate, 5 µg/ml insulin, 5 µg/ml human transferrin, 5 ng/ml sodium selenite and 200 nM dexamethasone. On Transwell filter inserts, a seeding density of 250,000 cells/cm^2 was used, otherwise 75,000 cells/cm^2.

2.3 Stable transfection with shRNA

Stably transfected cell lines were generated by Elena Schwagerus (Trinity College Dublin, Ireland).

To stably down-regulate δ-ENaC expression in H441 and Calu-3 cells, commercially available δ-ENaC shRNA lentiviral particles (SC-42421-V, Santa Cruz Biotechnology) were used. The particle pool consisted of transduction-ready viral particles carrying three different constructs, each encoding for a 19 nt shRNA (shRNA sequences given in **Table 1)**, designed to silence δ-ENaC gene expression, and a puromycin resistance gene. As negative control, control shRNA lentiviral particles (SC-108080, Santa Cruz), carrying constructs encoding for negative scrambled shRNA and puromycin resistance gene, were used. Cells (H441 passage 59, Calu-3 passage 38) were seeded at 100,000 cells/cm^2 in 24-well plates 24 h prior to lentiviral infection. The following day, medium was replaced by fresh medium containing 5 µg/ml Polybrene (Santa Cruz), a polycation, neutralising membrane charges and, hence, enhancing the interaction between the cell membrane and the viral capsid. Subsequently, lentiviral particles were added onto the cells (7.5×10^3 infectious units of virus (IFU) per well). Forty-eight hours after the transduction, cells were subcultured at a 1:3 ratio. Following overnight incubation in complete medium, puromycin containing medium was applied onto the cells to select stably shRNA expressing puromycin-resistant cells. The puromycin concentration suitable for selection was determined previously as the lowest concentration to kill 100% of wild-type cells in 3-5 days from the start of the puromycin selection and was 2.5 µg/ml puromycin for H441 and 7.5 µg/ml for Calu-3 cells. Subsequently, selected puromycin-resistant cells were expanded and, in the further course, are referred to as **H441 shDENaC,**

H441 shCTRL, Calu-3 shDENaC and **Calu-3 shCTRL** for H441 and Calu-3 cells transfected with δ-ENaC and scrambled shRNA, respectively.

shRNA	shRNA sequence (5' to 3')	
	Sense	**antisense**
A	GUG ACG AAG CUG UGA UUC Att	UGA AUC ACA GCU UCG UCA Ctt
B	CAC CUU CUU CUG CAC CAA Utt	AUU GGU GCA GAA GAA GGU Gtt
C	GGU ACC ACU UCC ACU AUG Utt	ACA UAG UGG AAG UGG UAC Ctt

Table 1

Nucleotide sequence of δ-ENaC shRNA constructs in δ-ENaC shRNA lentiviral particles (SC-42421-V, Santa Cruz Biotechnology, Heidelberg, Germany) according to manufacturer's product information.

2.4 Delta-ENaC over-expression studies

Transfections were carried out by Elena Schwagerus (Trinity College Dublin, Ireland).

2.4.1 Transient δ-ENaC over-expression

For transient overexpression, plasmid construct coding for human δ_1-ENaC protein subcloned in pcDNA3.1(+) vector, kindly provided by Dr. Diego Alvarez de la Rosa (Universidad de La Laguna, La Laguna, Spain), was used. Details on

generation and amplification of the plasmid are given below. H441 cells were transfected using Lipofectamine 2000 transfection reagent (Invitrogen) following manufacturer's protocol. Briefly, approx 90% confluent cell monolayers were transfected 24 h after seeding with a transfection mixture of 0.8 µg plasmid cDNA and 0.4, 2 and 4 µl Lipofectamine 2000 transfection reagent (1:0.5, 1:2.5 and 1:5 ratio of µg cDNA to µl Lipofectamine 2000) to optimise the transfection conditions. The Lipofectamine 2000/plasmid cDNA complexes remained on the cells for 24 h. Two hours after transfection, ENaC inhibitor benzamil was added to the medium at a concentration of 10 µM in order to prevent adverse effects of increased Na^+ influx on cell viability. Protein samples to assess δ-ENaC over-expression were collected 24, 48 and 72 h after transfection, quantified and analysed by Western blot. The transfection mixture with 1:5 ratio of µl cDNA to µl Lipofectamine 2000 was shown to result in the highest δ-ENaC over-expression levels and was used for all subsequent experiments as well as for generation of stably δ-ENaC over-expressing cell lines.

2.4.2 Stable δ-ENaC over-expression

H441 (passage 68) cells were transfected with a transfection mixture of 0.8 µg δ_1-ENaC plasmid cDNA and 4 µl Lipofectamine 2000. Two hours after transfection, 10 µM benzamil was added to the medium. Cells were subcultured into medium containing 600 µg/ml aminoglycoside antibiotic geneticin (G418, Sigma-Aldrich) and 10 µM benzamil in ratio 1:5 to 1:100 forty-eight hours after transfection. A G418 concentration of 600 µg/ml was previously shown to be suitable for selection. Subsequently, several G418-resistant colonies were picked, expanded and assessed for δ-ENaC expression by Western blot. Colonies stably

expressing δ-ENaC were kept in culture and used for the subsequent expression and functional studies. In further course, the generated stable cell line is referred to as **H441 DENaC**.

2.4.3 cDNA construct

Plasmid construct coding for full length δ_1-ENaC protein was kindly provided by Dr. Diego Alvarez de la Rosa (Universidad de La Laguna, La Laguna, Spain). Plasmid was generated, as described by Wesch *et al.* [59], by restriction enzyme subcloning of human δ_1-ENaC cDNA in pcDNA3.1(+) vector, and subsequently amplified by transformation in *Escherichia coli*. Briefly, 25 µl *E. coli* (Invitrogen) were transformed with 200 ng of the relevant plasmid cDNA and, following 1 h incubation in 200 µl SOC medium (Invitrogen) at 37°C, plated on Luria Bertani (LB) plates containing 50 µg/ml ampicillin. After overnight incubation at 37°C, 5 ml LB medium containing 50 µg/ml of ampicillin was inoculated with transformed *E. coli* and incubated for 12-16 h at 37°C with constant shaking. Subsequently, DNA was isolated using QIAprep Spin Miniprep Kit (Qiagen, Crawley, UK) and quantified with NanoDrop ND 1000 spectrophotometer (Labtech International, Ringmer, UK).

2.5 Western blot analysis

Unless mentioned otherwise, protein was isolated from confluent cell monolayers of H441 and Calu-3 cells on day 8 or 12 in culture, respectively. All steps were performed on ice. Cells were lysed using cell extraction buffer (Invitrogen), supplemented 1:100 with protease inhibitor cocktail (Sigma-Aldrich) and

subsequently sonicated for twice for 10 s to disrupt the cells. The lysates were then centrifuged for 20 min at 10,000 rpm at 4°C in order to remove the remaining cell debris. Supernatants were collected and used for further analysis. Protein concentrations were determined using a standard protein assay (Bio-Rad, Hemel Hempstead, UK) according to the manufacturer's instructions. A total of 50 µg of protein was loaded for each sample, after which samples were separated by sodium dodecyl sulphate polyacrylamide gel electrophoresis (SDS-PAGE, 8.5% acrylamide) and transferred to immunoblot polyvinylidene fluoride membranes (Bio-Rad). Non-specific binding sites were blocked with 5% bovine serum albumin (BSA) in Tris-buffered saline (0.1% Tween 20, pH 7.4) for 1 h at room temperature. Incubation with the relevant primary antibody was carried out overnight at 4°C. Following dilutions of primary antibodies in blocking buffer were used: 1:250 and 1:5,000 for anti-δ-ENaC antibodies (SC and DAR, respectively); 1:7,500 for anti-Na^+/K^+-ATPase, 1:8,000 for anti-β-actin. After washing with washing buffer (0.1% Tween 20 in Tris-buffered saline, pH 7.4), the membranes were incubated with the relevant HRP-conjugated secondary antibodies at the dilution 1:12,500 for 1 h at room temperature. Peroxidase activity was detected with Immobilon Western Chemiluminescent HRP substrate (Millipore). Using a Chemidoc documentation system (Bio-Rad), relative levels of protein expression were quantified by densitometric analysis of the immunoblot and normalisation to β-actin to ensure equal loading.

2.6 Cell surface biotinylation

Cells were grown on Transwell Clear inserts and used on day 8 (H441) or day 12 (Calu-3) in culture. All steps were performed on ice, using ice-cold solutions.

After both apical and basolateral sides of cell monolayers were rinsed with PBS containing 2.0 mM $CaCl_2$, 0.5 ml or 1.5 ml of biotinylation solution (0.5 mg/ml sulpho-NHS-biotin, 85 mM NaCl, 4 mM KCl, 15 mM $Na_2B_4O_7$, pH 9.0) were added to the apical or basolateral compartments, respectively. Phosphate buffered saline, supplemented with 2.0 mM $CaCl_2$ and 10% BSA, was applied to the respective opposite compartments, and cell monolayers were incubated with gentle agitation for 20 min at 4°C. A second 20 min incubation with 10% BSA in PBS, added to both compartments, followed to stop the biotinylation reaction. Subsequently, cells were treated with biotinylation lysis buffer (0.4% deoxycholate, 1% Triton X-100, 50 mM EGTA, 10 mM Tris-HCl, pH 7.4), supplemented with protease inhibitor cocktail (Sigma-Aldrich). To isolate the biotinylated membrane proteins, whole cell lysates were added to streptavidin-agarose beads (Sigma-Aldrich) and incubated overnight at 4°C. The following day, biotinylated proteins, now bound onto the beads, were separated from non-biotinylated proteins by centrifugation and extensive washing. Subsequently, biotinylated proteins were eluted by incubating the beads in 2x loading buffer at room temperature and at 95°C for 20 and 5 min, respectively. Apical and basolateral membrane proteins were then analysed by Western blot.

2.7 Protein deglycosylation

GlycoProfile II, Enzymatic In-Solution N-Deglycosylation kit (Sigma-Aldrich) was used according to manufacturer's instructions. Briefly, sample aliquot containing 50 µg protein was diluted to the total volume of 90 µl and denaturised by incubation with denaturant solution containing 2% octyl-β-D-glucopyranoside and 100 mM β-mercaptoethanol at 100°C for 10 min. Samples were then divided into

two aliquots. PNGase F Enzyme Solution was added to the test sample at the concentration of 50 units/ml. Equal volume of water was added to the untreated control sample. After 5 hours of incubation at 37°C, the reaction was stopped by heating at 100°C for 10 min.

PNGase F treated samples and untreated controls were subsequently analysed by Western blot.

2.8 Immunofluorescence microscopy (IFM)

Transwell filter grown cell monolayers were fixed by 10 min incubation with ice-cold methanol, followed by 8 min permeabilisation with 0.1% Triton X-100. Unspecific binding sites were blocked by incubation with PBS containing 5% BSA at 37°C for 30 min. After a 60 min incubation with 200 µl dilution of the respective primary antibody (δ-ENaC (SC), δ-ENaC (DAR) 1:50) in PBS containing 1% BSA, the cell layers were washed three times with PBS (1% BSA), before incubation with 200 µl of a 1:1000 dilution of the relevant Alexa Fluor-488-labelled $F(ab')_2$ fragment in PBS containing 1% BSA. To counterstain cell nuclei, propidium iodide (1 µg/ml in PBS) was used. After 30 min of incubation, the specimens were again washed three times with PBS (1% BSA) and embedded in FluorSave anti-fade medium (Merck, Nottingham, UK). Images were obtained using a confocal laser scanning microscope (CLSM, Zeiss LSM 510, Göttingen, Germany).

2.9 Ussing chamber experiments

Confluent cell monolayers grown on Transwell Clear filter inserts were mounted in custom-made, modified Ussing chambers. Both chamber compartments were

filled with Krebs-Ringer-Buffer pH 7.4 (116.4 mM NaCl, 5.4 mM KCl, 0.78 mM NaH_2PO_4, 25 mM $NaHCO_3$, 5.55 mM glucose, 15 mM HEPES, 1.8 mM $CaCl_2$, 0.81 mM $MgSO_4$). For a number of experiments with wild-type H441 cells, sodium-free KCl-Ringer-Buffer was also used (5.4 mM NaCl, 116.4 mM KCl, 0.78 mM KH_2PO_4, 25 mM $KHCO_3$, 1.8 mM $CaCl_2$, 0.81 $MgSO_4$, 5.55 mM glucose, 15 mM HEPES). Bathing solutions were continuously stirred and maintained at 37°C throughout the experiment.

For detection of electrical parameters, Ag/AgCl electrodes with KCl/agar bridges (3% agarose in 3 M KCl) were used to connect the chamber with the voltage-clamp amplifier. The transepithelial potential difference (V_t) was clamped to 0.0 mV and the short-circuit current (I_{SC}) was measured with DVC-1000 Dual voltage Clamp (World Precision Instruments, Sarasota, FL). To monitor the transepithelial electrical resistance, voltage pulses of 0.5 mV were applied for duration of 5 s every 50 s. The I_{SC} was continuously recorded using Chart5 for Windows software (ADInstruments, Oxfordshire, UK).

After a stable basal I_{SC} was reached (after approximately 10-15 min), chemical compounds were applied. Stock solutions of 50 mM Evans blue, 5 mM capsazepine, 10 mM icilin, 50 mM amiloride and 100 mM ouabain, all dissolved in DMSO, were used (all from Sigma-Aldrich).

Ussing chamber studies with Calu-3 monolayers, wild-type as well as transfectants, were carried out between day 14 and 21 in culture (Calu-3: passage 39, 45, 47; Calu-3 shCTRL: passage 46, 48, 59; Calu-3 shDENAC: passage 47, 48, 60). H441 cells were used on day 8 to 14 in culture (H441: passage 63 – 65; H441 shCTRL: passage 67, 69, 70; H441 shDENAC: passage

67, 69, 70; H441 DENaC: passage (+8) – (+12)). Cell monolayers were only used if the transepithelial electrical resistance reached a value of at least 400 Ω•cm^2.

2.10 Patch-clamp recordings

Patch-clamp studies were performed using δ-ENaC over-expressing H441 cells in the whole-cell configuration (passages (+8) – (+12)). Cells were seeded on Petri-dishes (diameter 35 mm) in H441 cell culture medium containing 600 µg/ml G418 and 10 µM benzamil 24 h prior to the experiments.

	Bath solution	**Pipette Solution**
NaCl	140	-
CsCl	-	140
$CaCl_2$	2	-
$MgCl_2$	1	1
EGTA	-	5
HEPES	10	10

Table 2

Patch-clamp solutions (concentrations in mM).

Borosilicate glass capillaries (Harvard Apparatus, Edenbridge, UK) were pulled to patch electrodes (2–4 MΩ resistance) using a DMZ-universal-puller (Zeitz-Instruments, Munich, Germany) and back-filled with pipette solution (pH 7.4; 280 mOsm/kg H_2O). Cells were first rinsed and then continuously perfused with bath solution (pH 7.4; 300-310 mOsm/kg H_2O) (**Table 2**).

After selecting a cell for recording, the pipette was introduced into the bath solution, and the current offset was adjusted to zero. By gently pressing the pipette against the cell surface and applying slight negative pressure, a seal of more than 10 GΩ resistance was formed. Steadily increased suction was applied to break into the whole-cell mode. The access resistance was kept as low as possible (R_a < 15 MΩ). The holding potential was clamped to -60 mV. Currents were amplified with Axopatch 200B amplifier, sampled at 2 kHz using Digidata 1322A and recorded using Clampex software (all from Axon instruments, Jakarta, Indonesia). Data analysis was carried out using Clampfit 9.2 software (Axon instruments).

After the currents in whole cell mode stabilised, 10 μM amiloride were added to determine the portion of amiloride-sensitive (and α-ENaC-mediated) current. Subsequently, cells were perfused with bath solution to reverse the inhibition by amiloride, and 20 μM capsazepine were added. Finally, cells were perfused with the bathing solution containing both 10 μM amiloride and 20 μM capsazepine in order to evaluate the percentage of amiloride-sensitive currents off the capsazepine-induced effect.

2.11 Statistical analysis

Each experiment was carried out at least in triplicate using cells from different passages and results were expressed as means ± SD unless mentioned otherwise. Two groups were compared using one-way analysis of variance (ANOVA), followed by the Student–Newman–Keuls post-hoc test. $P < 0.05$ was considered as significant.

3 RESULTS

3.1 Sodium-dependence of the pharmacological responses to the alleged δ-ENaC modulators in H441 cells

A side project of this thesis was concerned with determining the sodium-dependence of effects caused by the respective activators and inhibitors of δ-ENaC function in H441 cells. To this end, Ussing chamber experiments were carried out in KRB and also in the corresponding sodium-free buffer.

To estimate the integrity of the cell monolayer, the transepithelial electrical resistance (TEER) values of cells grown on permeable filter supports were measured every other day. Only monolayers with resistances exceeding 400 $\Omega \bullet cm^2$ were used for Ussing chamber studies. H441 cells grown on Transwell Clear inserts developed TEER values > 400 $\Omega \bullet cm^2$ by day 6 in culture (**Figure 7**).

The average basal I_{SC} was 4.7 ± 1.4 $\mu A/cm^2$ (*n* = 10) in KRB. In sodium-free buffer, cell monolayers displayed initial I_{SC} values of 0.2 ± 0.7 $\mu A/cm^2$ (*n* = 10).

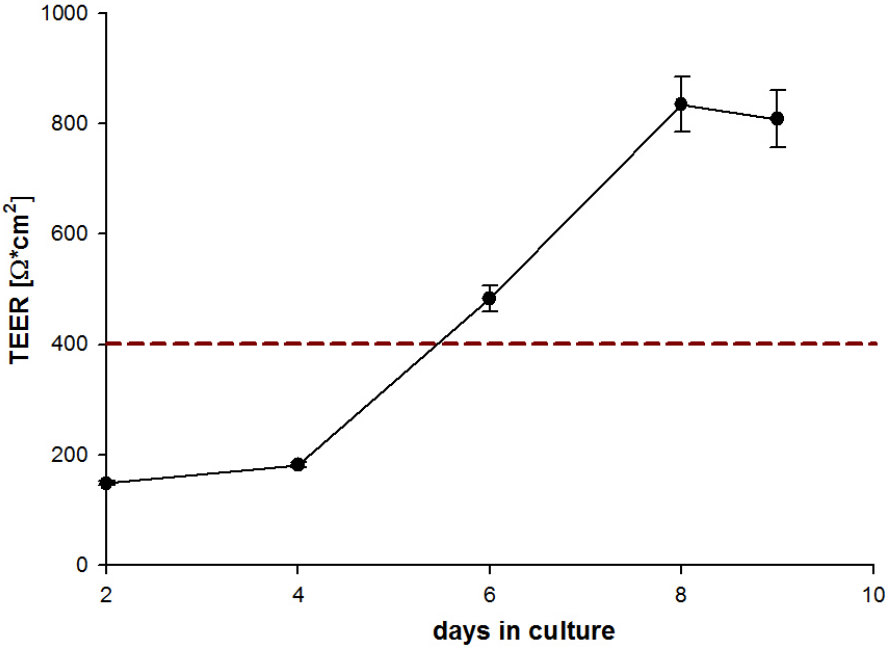

Figure 7

Transepithelial electrical resistances of H441 wt (passage 61) cell monolayers grown on permeable filter inserts in course of the time in culture. Red dotted line symbolises TEER of 400 Ω•cm^2. Results are expressed as means ± SD (*n* = 6).

Figure 8 presents representative current traces of H441 wt cells in response to administration of Evans blue (EB), capsazepine and icilin in KRB and sodium-free buffer, respectively.

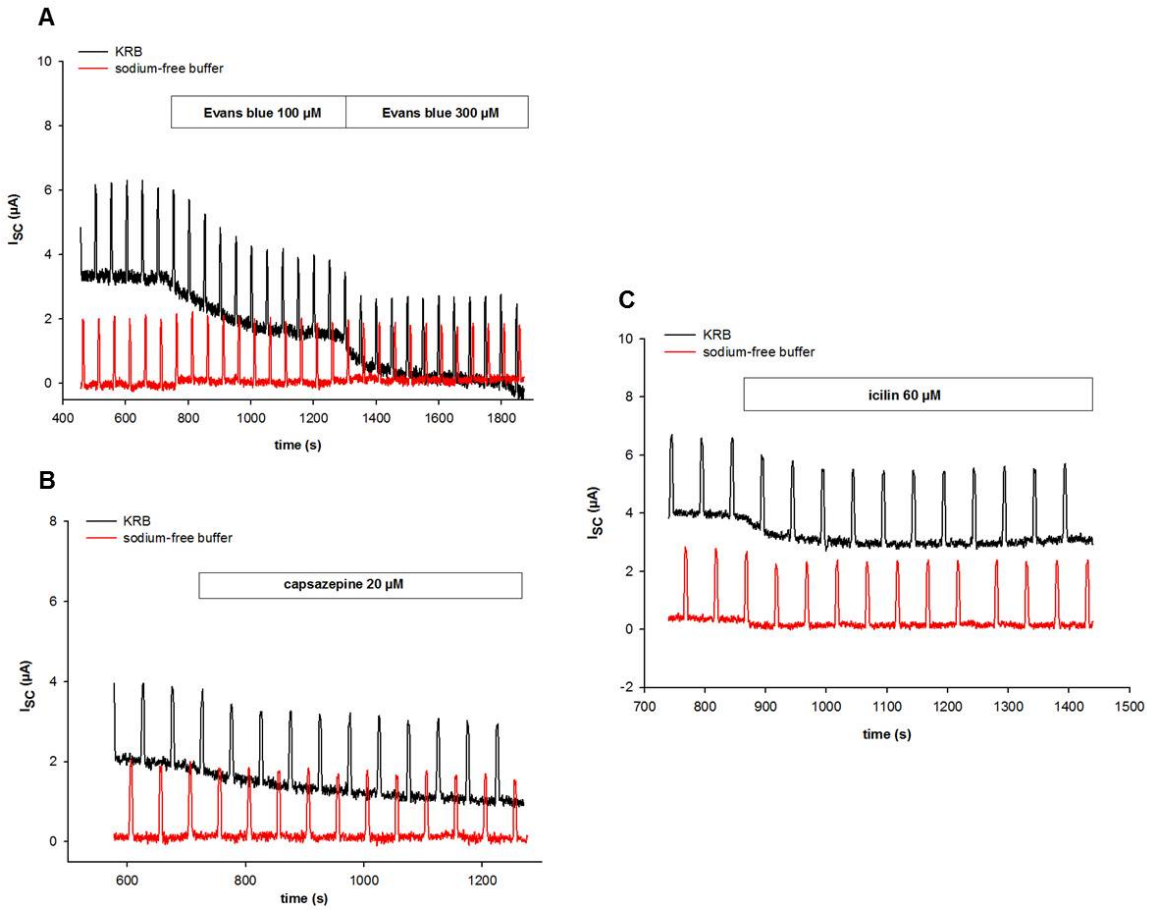

Figure 8

Sodium-dependence of the apical responses to EB, capsazepine and icilin in H441 cell monolayers. Comparison of the representative current traces, obtained after application of 100 µM and 300 µM EB **(A)**, 20 µM capsazepine **(B)** and 60 µM icilin **(C)** to the H441 cell monolayers in KRB (black line) and in sodium-free buffer (red line).

In the absence of sodium, adding 100 µM EB to the H441 cell monolayers had an effect of 0.02 ± 0.18 µA/cm^2 (n = 4). Addition of 300 µM EB resulted in a change of the I_{SC} of -0.07 ± 0.30 µA/cm^2 (n = 4). The change in I_{SC} in both cases was negligible and significantly different from the effect in KRB (i.e., 100 µM EB: -2.3 ± 1.2 µA/cm^2; 300 µM EB: -3.3 ± 1.3 µA/cm^2) (P < 0.01) **(Figure 9)**.

When applied apically, 20 µM capsazepine resulted in a decrease in I_{SC} of 0.04 ± 0.06 µA/cm^2 (*n* = 3). In contrast, the I_{SC} decrease in KRB accounted for 1.0 ± 0.8 µA/cm^2 (*n* = 3). However, due to the high standard deviation, the difference in the amplitudes of the capsazepine-effects in KRB and sodium-free medium was not significant.

The application of 60 µM icilin in the absence of sodium ions led to the most pronounced effect, compared to the effects of EB and capsazepine in the sodium-free buffer. Short-circuit currents were decreased by 0.17 ± 0.15 µA/cm^2 (*n* = 3). Nevertheless, the amplitude of the decrease was significantly smaller than in KRB (1.1 ± 0.4) (*P* < 0.05).

In summary, effects observed in sodium-free buffer did not represent significant changes of I_{SC} compared to the baseline level. In contrast, in KRB, addition of Evans blue, capsazepine and icilin affected the short-circuit currents across H441 cell monolayers significantly. **Figure 9** demonstrates the differences in the effects observed in KRB and in sodium-free buffer.

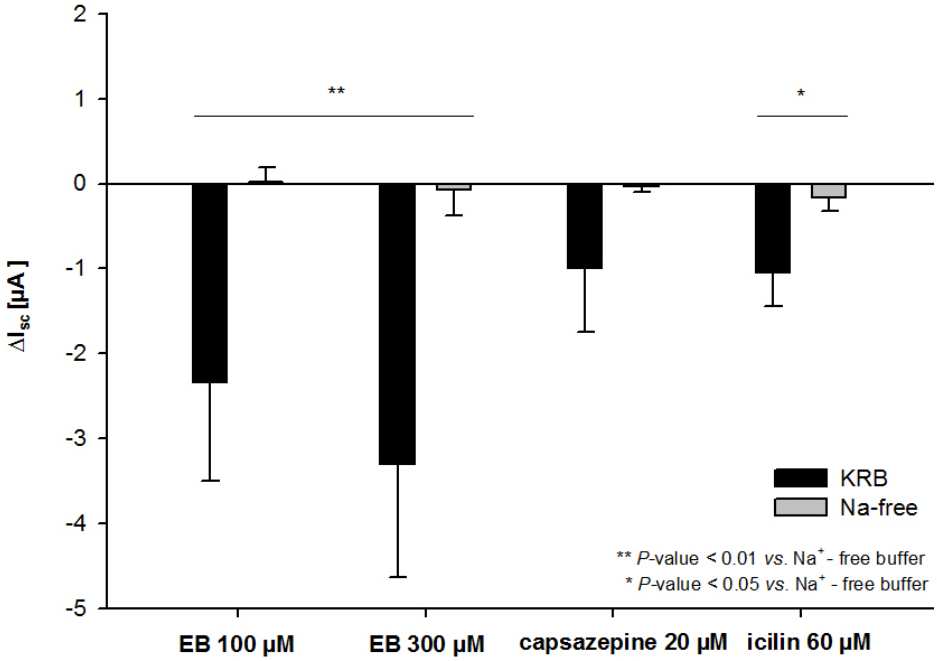

Figure 9

Sodium-dependence of apical response to 100 μM and 300 μM Evans blue, 20 μM capsazepine and 60 μM icilin in H441 cell monolayers. Results are expressed as means ± SD (*n* = 3-4). The statistical significance of the difference is expressed as **, *P* < 0.01 and *, *P* < 0.05 versus the compounds' effects in sodium-free buffer.

3.2 Stable knock-down of the δ-ENaC subunit in H441 and Calu-3 cells using shRNA

The effects of the δ-ENaC modulators had previously been investigated in Dr. Ehrhardt's lab. Since they were different from published data [21, 47, 54, 58], my aim was to determine the δ-ENaC specificity of the observed effects by knocking-down the δ-ENaC protein.

3.2.1 Western blot studies – monitoring changes in the δ-ENaC expression on protein level

For the densitometric quantification, the bands at 100 kDa and 70 kDa were analysed. Beta-actin was used as loading control.

3.2.1.1 H441

When incubated with the SC antibody, H441 immunoblots revealed a prominent band above 70 kDa, resembling the calculated molecular weight of the δ-ENaC protein, a much fainter band at 100 kDa, corresponding to the δ-ENaC protein according to the manufacturer's specifications, as well as multiple protein bands at lower molecular weights (**Figure 10 (A)**).

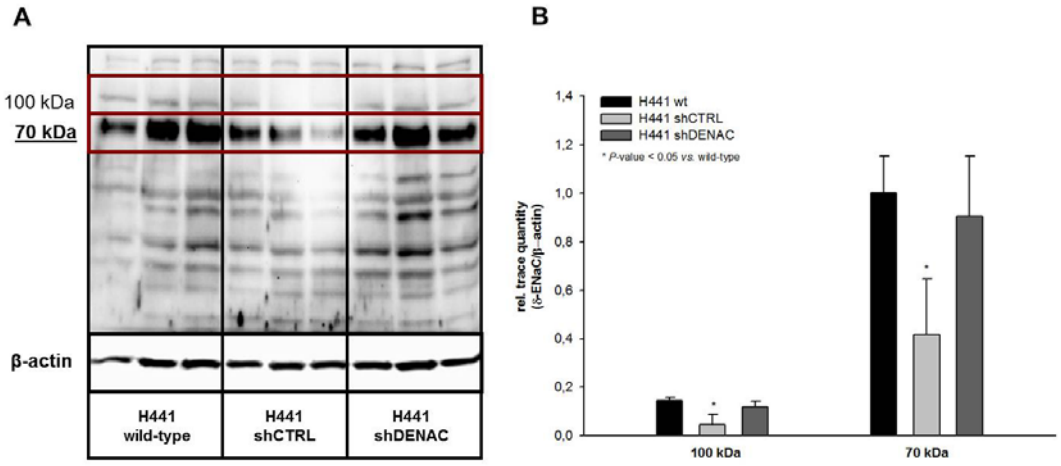

Figure 10

(A) Western blot of lysates from H441 wild-type, shCTRL and shDENAC cells, probed with anti-δ-ENaC SC antibody (3 lanes represent protein isolations from 3 different passages) **(B)** Densitometric analysis of δ-ENaC protein bands detected at 70 and 100 kDa relative to β-actin (means ± SD, $n = 3$). *, $P < 0.05$ *vs.* relative signal intensity of the respective bands in the wild-type cells.

The densitometric quantification of protein band intensities at both 70 kDa and 100 kDa (**Figure 10 (B)**) suggested a significant decrease in δ-ENaC abundance in mock-transfected H441 cells (H441 shCTRL), when compared to the expression levels in the wild-type cells. However, no significant decrease was observed in δ-ENaC knockdown transfectants (H441 shDENAC). It was rather the case that H441 shDENaC transfectants showed higher δ-ENaC expression than the H441 shCTRL cells. This observation could potentially be explained by incomplete blotting of the mock-transfected samples, as seen in **Figure 10 (A)**.

In contrast, in Western blots incubated with DAR antibody distinctive bands at 100 kDa, but only very faint bands at 70 kDa (**Figure 11 A**) were observed.

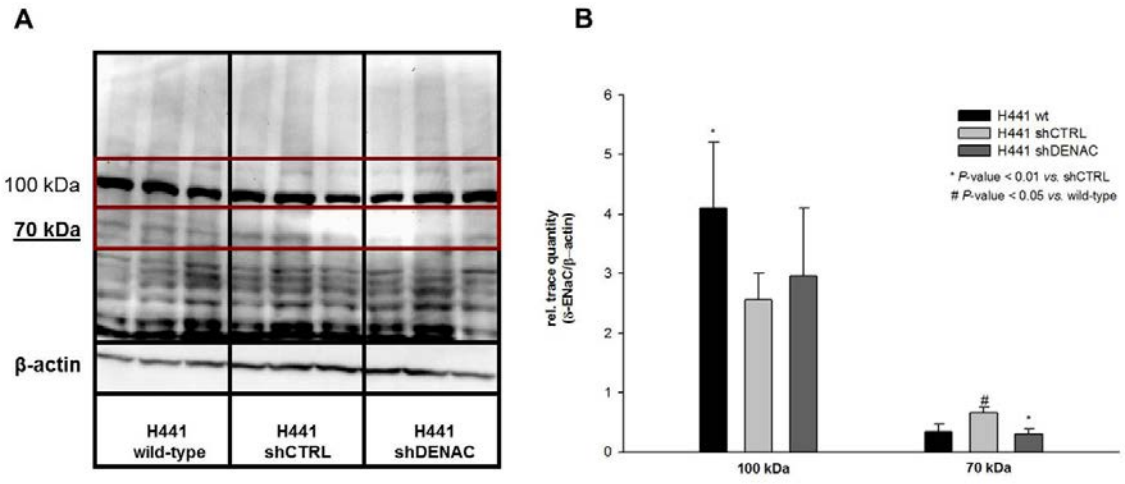

Figure 11

(A) Western blot of lysates from H441 wild-type, shCTRL and shDENAC cells, probed with anti-δ-ENaC DAR antibody (3 lanes represent protein isolations from 3 different passages). **(B)** Densitometric analysis of δ-ENaC protein bands detected at 70 and 100 kDa relative to β-actin (means ± SD, $n = 3$). #, $P < 0.05$ *vs.* relative signal intensity of the respective bands in the wild-type cells; * $P < 0.01$ *vs.* H441 shCTRL cells.

As presented in **Figure 11 (B)**, there was a significant decrease in the intensity of the 100 kDa band in H441 shCTRL, when compared to H441 wt samples. However, a significant increase in the band intensity was observed at 70 kDa, when shCTRL samples were compared to both wild-type and shDENaC H441 samples. Again, these significant differences are more likely to be due to insufficient blotting rather than to a decrease in protein expression levels.

Densitometric analysis did not indicate a significant decrease in the protein expression of δ-ENaC in H441 shDENAC cells compared to the wild-type H441 cells, regardless of the antibody used and the molecular weight of the band analysed.

3.2.1.2 Calu-3

In respect of protein band patterns as well as of signal intensities detected at 70 kDa and 100 kDa, immunoblots of Calu-3 cell lysates were similar to those of H441 cells, obtained with both SC and DAR antibodies (**Figure 12 (A/C)**).

Using SC antibody, no significant differences in δ-ENaC protein expression were observed in Calu-3 shDENAC cells compared to the wild-type, at either of the molecular weights analysed (70 kDa and 100 kDa) (**Figure 12 (B)**).

Figure 12 (D) indicates significant increases of band intensities at 100 kDa (Calu-3 shCTRL) and at 70 kDa (Calu-3 shDENAC) compared to the respective signals in the wild-type cells. However, no reduction of protein expression in δ-ENaC shRNA transfected Calu-3 cells (shDENaC) was detected.

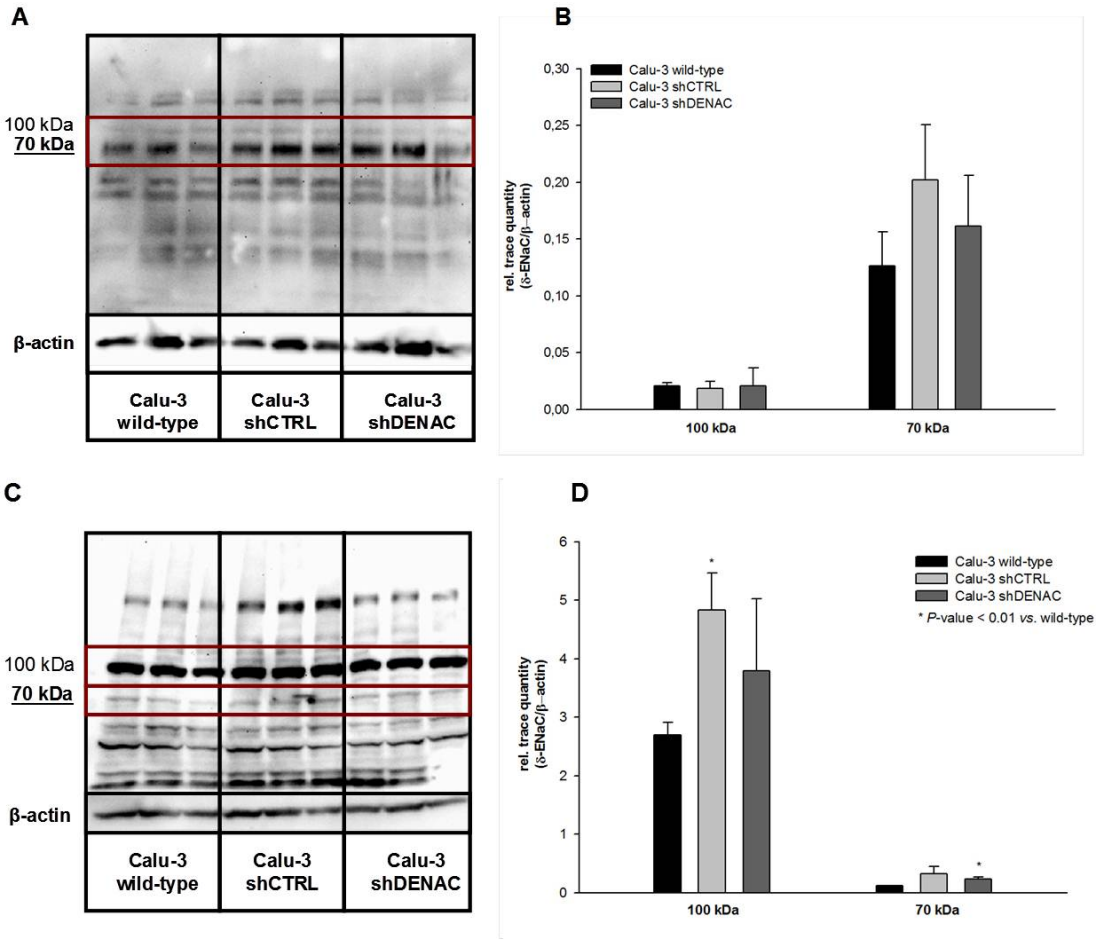

Figure 12

Western blot of cell lysates from Calu-3 wt, Calu-3 shCTRL and Calu-3 shDENAC cells, probed with anti-δ-ENaC SC **(A)** and DAR **(C)** antibodies (3 lanes represent protein isolations from 3 different passages). Densitometric analysis of δ-ENaC protein bands, detected at 70 and 100 kDa using SC and DAR antibodies (**(B)** and **(D)**, respectively), relative to β-actin (means ± SD, n = 3). *, $P < 0.01$ *vs.* relative signal intensity of the respective bands in the wild-type cells.

3.2.2 Ussing chamber studies – monitoring the knock-down of δ-ENaC expression on the functional level

After mounting cell monolayers grown on Transwell filter inserts into the Ussing chambers and stabilisation of the I_{SC}, Evans blue, capsazepine and icilin were

applied apically to the cell monolayers. In the cells stably transfected with δ-ENaC shRNA, the responses to the administration of the compounds were expected to be of smaller amplitude than in the wild-type and mock-transfected cells, due to down-regulated δ-ENaC expression levels, under assumption that the effects were δ-ENaC-specific and δ-ENaC knock-down was sufficient. The responses in the wild-type and mock-transfected cells were expected to be of comparable amplitudes.

3.2.2.1 Calu-3

Calu-3 cells grown on Transwell Clear inserts developed TEER values > 400 Ω•cm^2 by day 5-6 in culture, as shown in **Figure 13**, and were used on days 14 to 21, when TEER values peaked. There was no relevant difference in TEER values between Calu-3 wt, Calu-3 shCTRL and Calu-3 shDENAC cells.

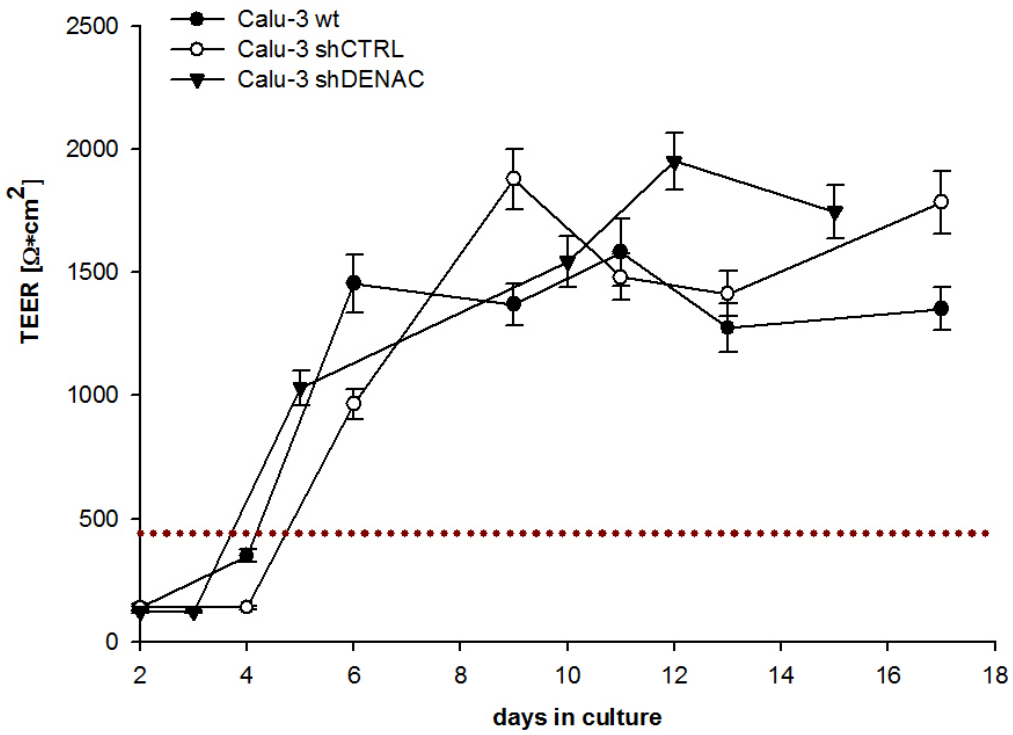

Figure 13

Transepithelial electrical resistances of Calu-3 wt (passage 45), Calu-3 shCTRL (passage 46) and Calu-3 shDENAC (passage 48) cell monolayers grown on permeable filter inserts in course of the time in culture. Red dotted line symbolises TEER of 400 Ω•cm^2. Results are expressed as means ± SD (*n* = 6).

Before adding the respective compound to the cell monolayers, the baseline short-circuit current value (I_{SC}) was given time (~10 min) to stabilise. The average steady state baseline I_{SC} was determined for Calu-3 wt, Calu-3 shCTRL and Calu-3 shDENAC cells and did not differ significantly between the cell types **(Figure 14)**.

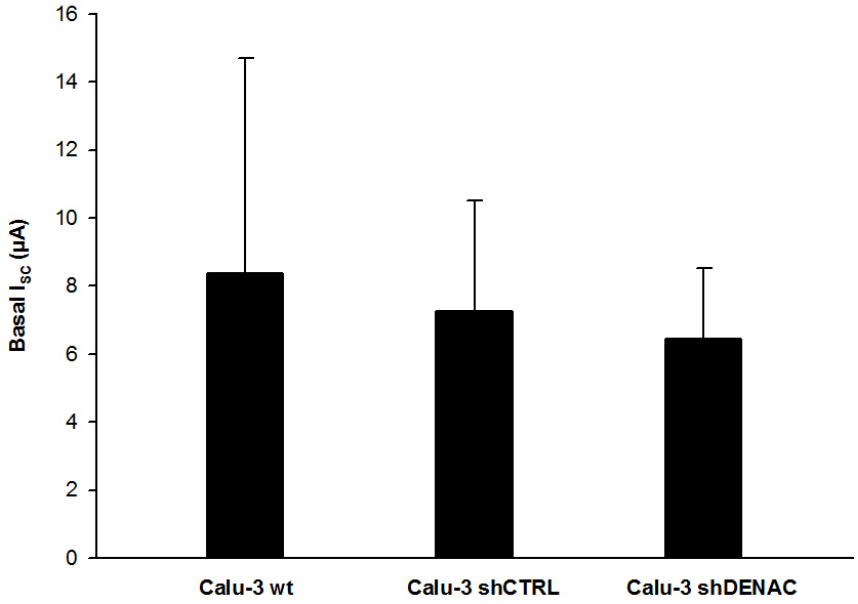

Figure 14

Steady state short-circuit current values (basal I_{SC} [µA]) of Calu-3 wt, Calu-3 shCTRL and Calu-3 shDENAC cell monolayers, obtained under standard conditions (apical and basolateral KRB; pH = 7.4) prior to the start of the measurements. Results are expressed as means ± SD (*n* = 10).

Response to apical application of Evans blue

Despite the fact that Evans blue (EB) has been stated to be a selective antagonist of δ-ENaC [47], it increased the I_{SC} levels in Calu-3 cell monolayers. **Figure 15 (A)** shows typical I_{SC} traces obtained in Calu-3 wild-type (black graph), Calu-3 shCTRL (red graph) and Calu-3 shDENAC (blue graph) cells after administration of 100 µM and 300 µM EB.

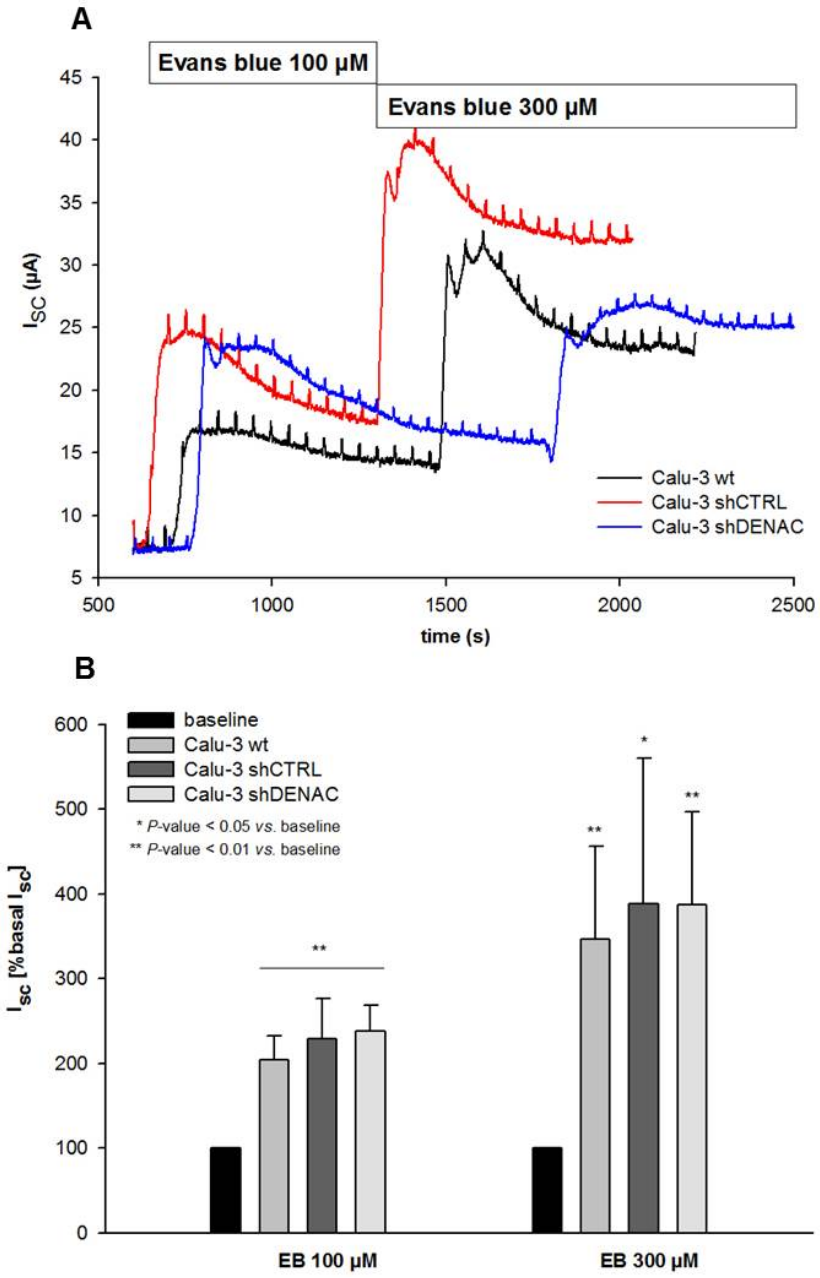

Figure 15

(A) Overlay of the representative current traces obtained in response to 100 µM and 300 µM Evans blue in the wild-type (wt, black line) and mock-transfected (shCTRL, red line) Calu-3 cells as well as in the cells transfected with δ-ENaC shRNA (shDENAC, blue line).

(B) Effects of apically administered Evans blue in Calu-3 wt, shCTRL and shDENAC cells. Short-circuit current values were measured 10 min after adding 100 and 300 µM of Evans blue and normalised to the baseline I_{SC} (100%). Results are expressed as means ± SD (*n* = 3 - 4). *, $P < 0.05$ *vs.* baseline; **, $P < 0.01$ *vs.* baseline.

Apical administration of 100 µM EB increased the I_{SC} of Calu-3 wild-type cell monolayers by 103.8 ± 28.5% (*n* = 4). Increases by 131.1 ± 47.4% (*n* = 3) and 137.9 ± 31.0% (*n* = 4) were observed in Calu-3 shCTRL and Calu-3 shDENAC cells, respectively (**Figure 15 (B)**). In all cases, the resulting I_{SC} levels were significantly different from the baseline ($P < 0.01$).

There was an additional significant increase in the I_{SC} resulting from the application of 300 µM EB, i.e., by 264.7 ± 109.7% of the baseline level in Calu-3 wt (*n* = 4; $P < 0.01$), by 300.0 ± 172.6% in Calu-3 shCTRL (*n* = 3; $P < 0.05$) and by 287.9 ± 108.7% in Calu-3 shDENAC cells (*n* = 3; $P < 0.01$). Hence, short-circuit current stimulation by EB was concentration-dependent in all cell types.

Response to apical application of capsazepine

Interestingly, the selective activator of δ-ENaC function, capsazepine [54], did not increase the I_{SC}, but to the contrary had an inhibitory effect on the currents in Calu-3 cells, as shown in **Figure 16 (A)**.

Whilst the I_{SC} decrease was significant in Calu-3 wt cells (14.7 ± 1.7% of the basal I_{SC}; *n* = 4; $P < 0.01$), currents were also inhibited in the mock-transfected and δ-ENaC shRNA transfected cells, however, not significantly due to a small number of replicates and a rather high standard deviation (*n* = 4) **(Figure 16 (B))**.

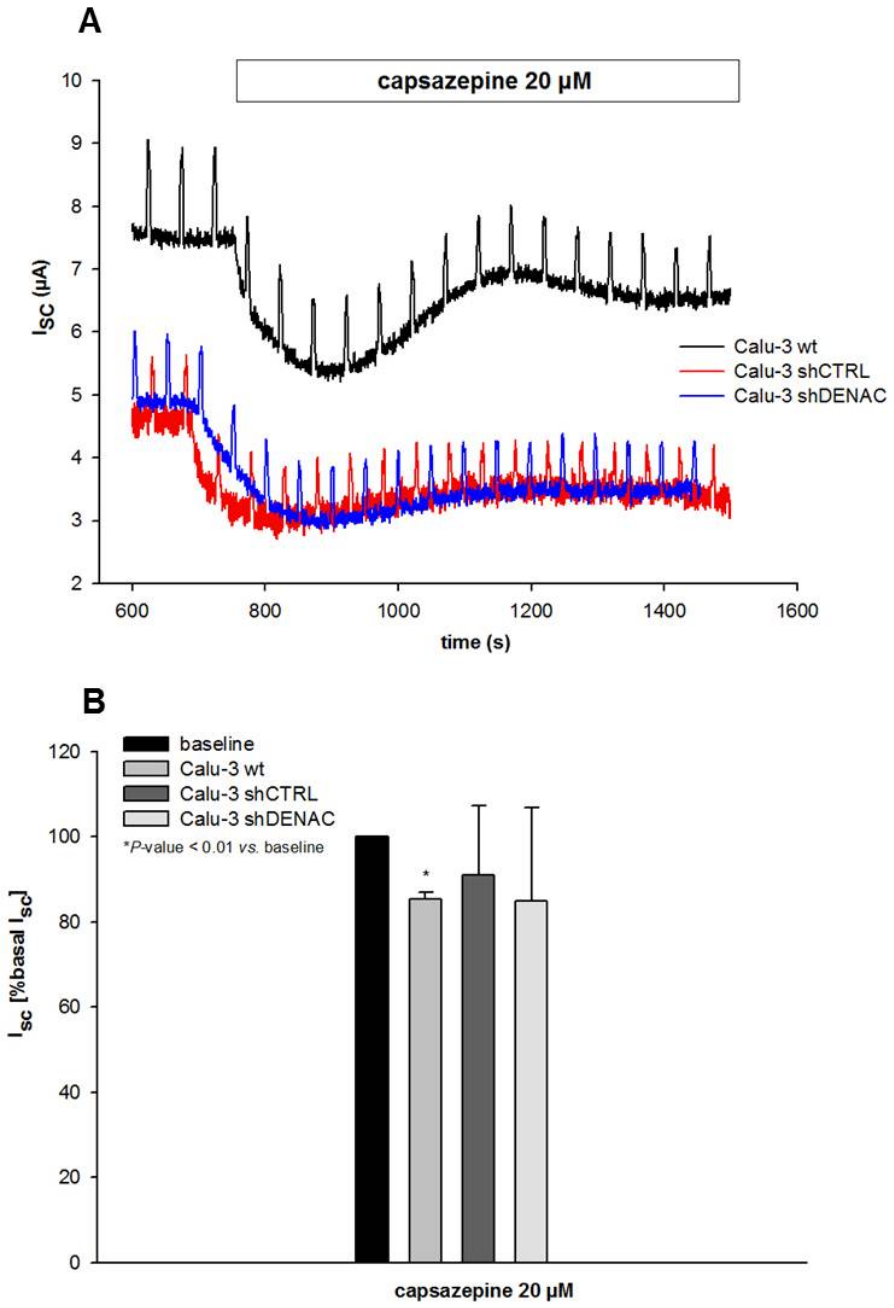

Figure 16

(A) Overlay of the current traces in response to addition of 20 µM capsazepine, obtained during representative Ussing chamber experiments in Calu-3 wild-type (black line), Calu-3 shCTRL (red line) and Calu-3 shDENAC cells (blue line).

(B) Effects of apically administered capsazepine (20 µM) in Calu-3 wt, shCTRL and shDENAC cells. Short-circuit current values were measured 10 min after adding the compound and normalised to the baseline I_{SC} (100%). Results are expressed as means ± SD (n = 4). *, $P < 0.01$ *vs.* baseline.

Response to apical application of icilin

Icilin has been described to be a selective activator of δ-ENAC function [58]. Indeed, the compound stimulated currents across the monolayers of Calu-3 wt cells as well as of the respective control- and knock-down-transfectants (**Figure 17 (A)**).

Administration of 60 µM icilin led to significant increases in the I_{SC} in Calu-3 wt and in Calu-3 shDENAC cells, by 47.6 ± 8.8% (*n* = 3) and 47.6 ± 12.2% (*n* = 5) of the baseline level, respectively. In Calu-3 shCTRL cells, the increase by 64.2 ± 53.1% (*n* = 4) was not significant due to the high standard deviation (**Figure 17 (B)**).

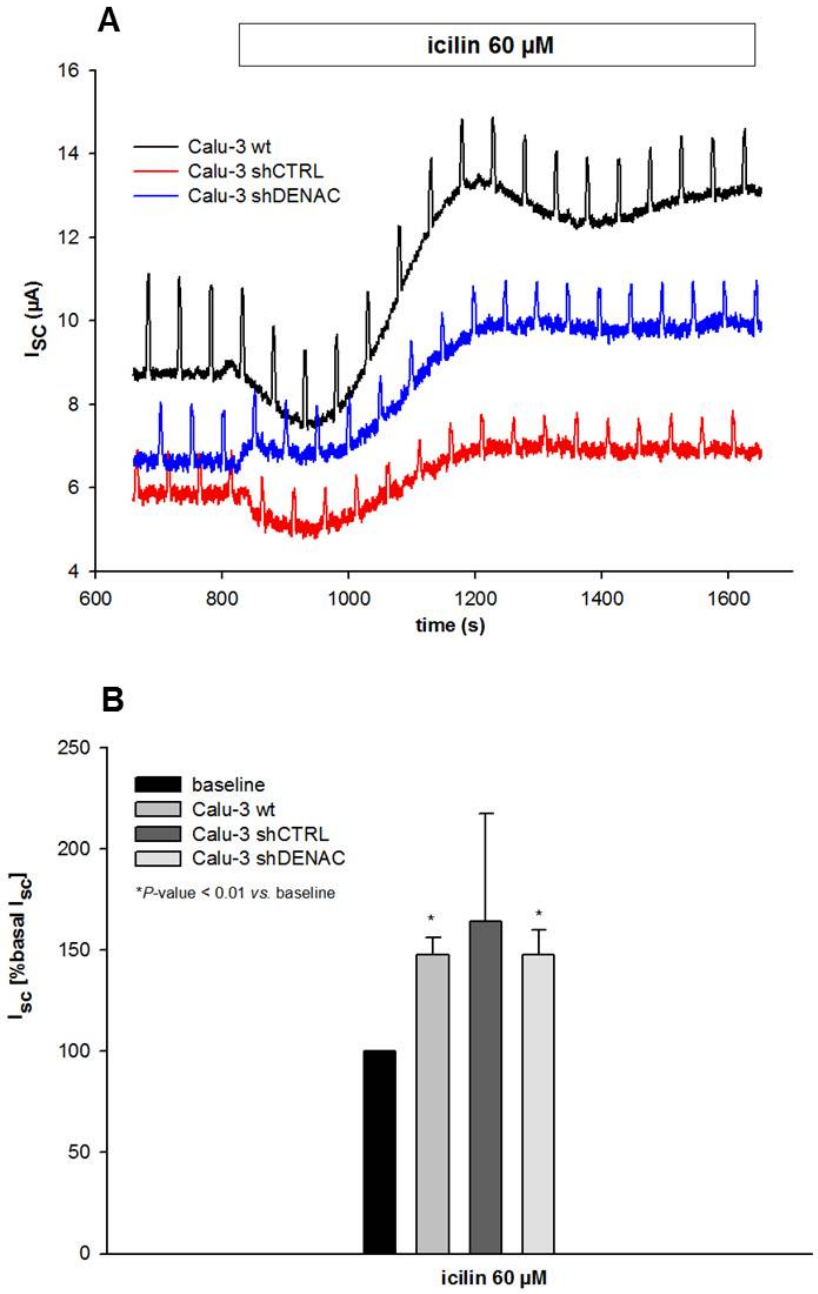

Figure 17

(A) Overlay of the representative current traces obtained in response to 60 µM icilin in Calu-3 wild type (black line), Calu-3 shCTRL (red line) and Calu-3 shDENAC cells (blue line).

(B) Effects of apically administered icilin (60 µM) in Calu-3 wt, shCTRL and shDENaC cell monolayers. Short-circuit current values were measured 10 min after adding the compound and normalised to the baseline I_{SC} (100%). Results are expressed as means ± SD (n = 3 - 5). *, $P < 0.01$ *vs.* baseline.

Comparison of the effects exhibited by the alleged modulators of δ-ENaC function in the wild-type, mock-transfected as well as in δ-ENaC shRNA transfected Calu-3 cells

Figure 18 summarises and compares the effects induced by Evans blue, capsazepine and icilin on the short-circuit currents in the wild-type (wt), mock-transfected (shCTRL) as well as δ-ENaC shRNA transfected (shDENAC) Calu-3 cells.

No significant difference in effects was observed between the mock-transfected Calu-3 shCTRL and Calu-3 shDENAC cells, suggesting that higher amplitude of the I_{SC} activation by EB in Calu-3 shCTRL and shDENAC cells could be due to the transfection procedure as such, rather than to down-regulation of δ-ENaC.

The observed inhibitory effects in response to administration of capsazepine did not differ significantly between the non-transfected Calu-3 cells and both transfectant types. Similarly, no significant difference in icilin-induced current activation was observed between Calu-3 wt, shCTRL and shDENaC cells.

In summary, no significant differences in pharmacological responses to administration of either of the compounds were detected between the wild-type, mock-transfected and δ-ENaC shRNA transfected Calu-3 cells.

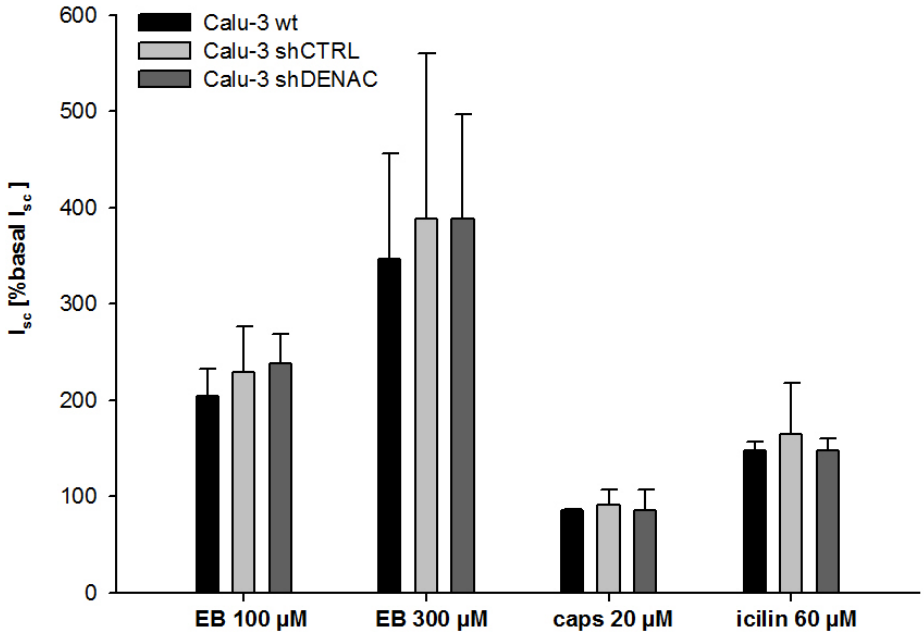

Figure 18

Quantification of responses to 100 µM and 300 µM Evans blue, 20 µM capsazepine and 60 µM icilin in Calu-3 cell monolayers of non-transfected cells (wt) as well as of cells, stably transfected with scrambled shRNA (shCTRL) and shRNA, designed to silence δ-ENaC (shDENAC). Short-circuit currents values, measured after the administration of the relevant compound, were normalised to the basal I_{SC}. Results are expressed as means ± SD (*n* = 3).

3.2.2.2 H441

As shown in **Figure 19,** H441 cells reached TEER values over 400 Ω•cm^2 by day 6 in culture. Transfected cells required approximately 9 days until they reached TEER levels > 400 Ω•cm^2. H441 cells were used for Ussing chamber experiments between day 7 and day 14 in culture when TEER values peaked.

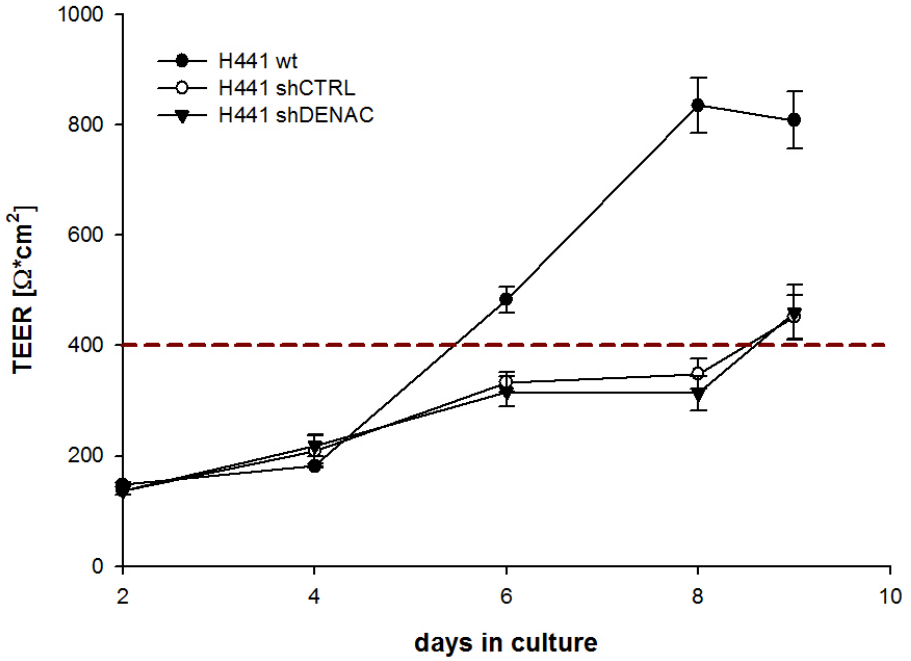

Figure 19

Transepithelial electrical resistance of H441 wt (passage 61), H441 shCTRL (passage 67) and H441 shDENAC (passage 67) cell monolayers grown on permeable filter inserts in course of the time in culture. Red dotted line symbolises TEER of 400 Ω•cm^2. Results are expressed as means ± SD (*n* = 6).

The basal I_{SC} of H441 wt monolayers stabilised on an average level of 4.2 ± 1.2 µA (*n* = 10), whereas the basal I_{SC} of H441 shCTRL and H441 shDENAC monolayers were significantly higher (7.8 ± 2.8 µA and 9.6 ± 5.7 µA, respectively; *n* = 10; *P* < 0.01) (**Figure 20**). However, there was no significant difference between the baseline I_{SC} levels of H441 shCTRL and H441 shDENAC cells.

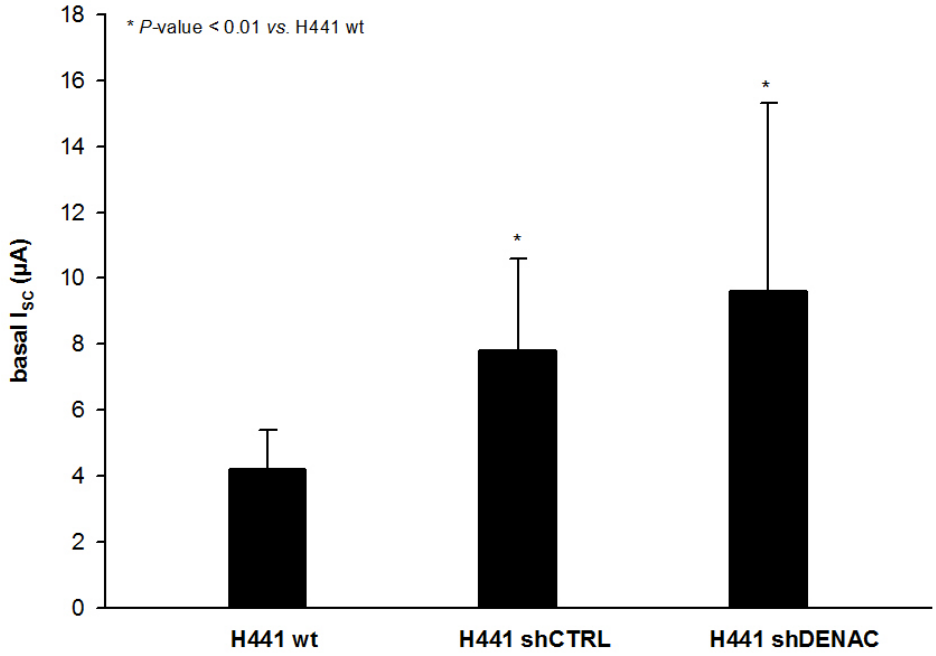

Figure 20

Steady state short-circuit current values (basal I_{SC} [µA]) of H441 wt, H441 shCTRL and H441 shDENAC cell monolayers, obtained under standard conditions (apical and basolateral KRB; pH = 7.4) prior to the start of the measurements. Results are expressed as means ± SD (*n* = 10). **, *P* < 0.01 *vs.* basal I_{SC} of the wild-type cells.

Response to apical application of Evans blue

Evans blue, which has been suggested as a selective δ-ENaC antagonist [47], decreased the I_{SC} of H441 cells in a concentration-dependent manner. **Figure 21 (A)** shows typical I_{SC} traces of H441 wild type (black line), H441 shCTRL (red line) and H441 shDENAC (blue line) cells in response to the administration of 100 µM and 300 µM of Evans blue.

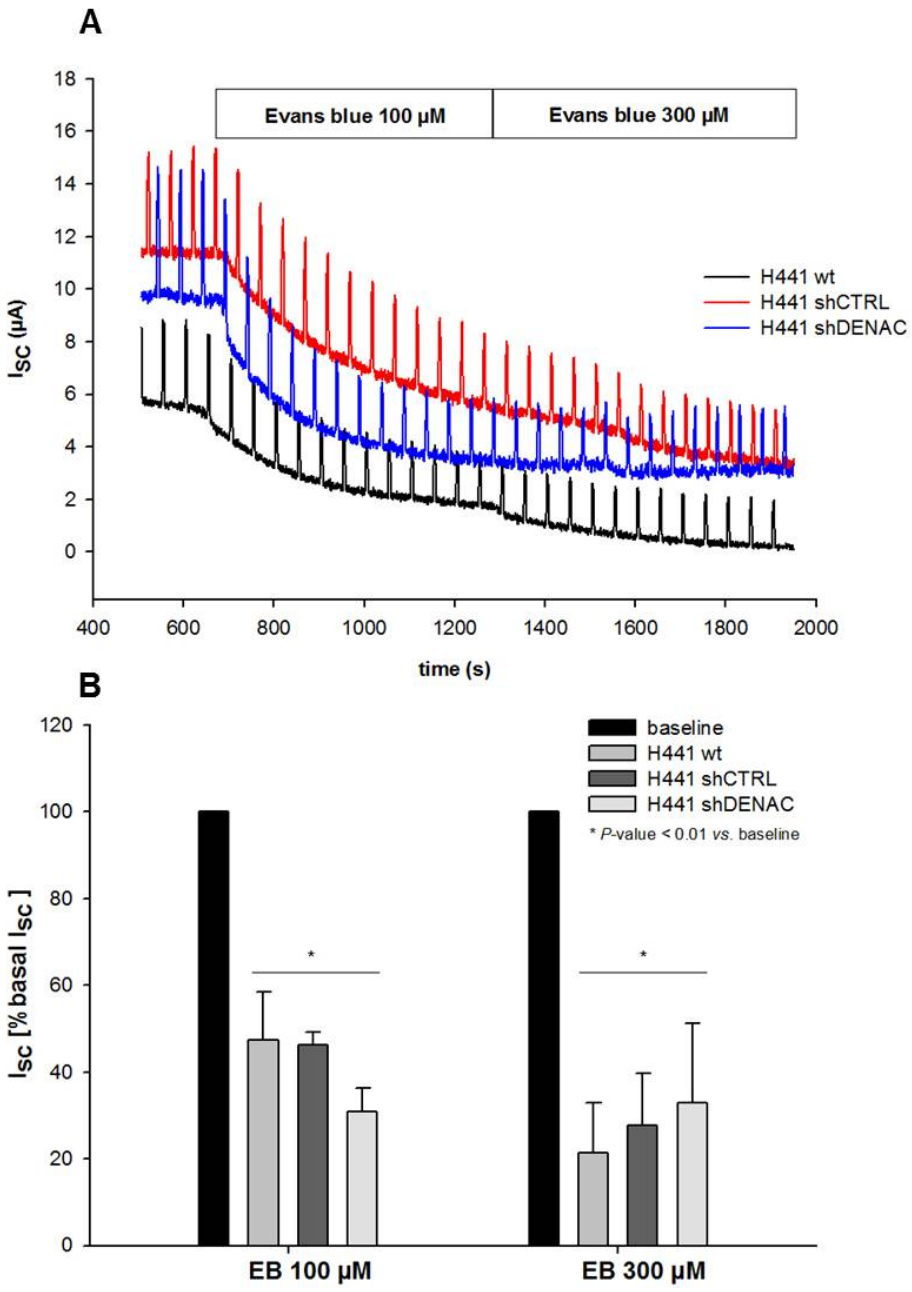

Figure 21

(A) Overlay of the representative current traces obtained in response to 100 µM and 300 µM Evans blue in the wild-type (wt, black line) and mock-transfected (shCTRL, red line) H441 cells as well as in the cells transfected with δ-ENaC shRNA (shDENAC, blue line).

(B) Effects of apically administered Evans blue in H441 wt, shCTRL and shDENAC cells. Short-circuit current values were measured 10 min after adding 100 and 300 µM of Evans blue and normalised to the baseline I_{SC} (100%). Results are expressed as means ± SD (n = 4). *, $P < 0.01$ *vs.* baseline.

More precisely (**Figure 21 (B)**), application of 100 µM Evans blue led to a significant decrease in the I_{SC} in H441 wt and H441 shCTRL cells, by 47.4 ± 11.0% and 46.2 ± 2.9% of the basal I_{SC} (n = 4; P < 0.01), respectively. After administration of 300 µM Evans blue, a further significant reduction of I_{SC} was observed, with the resulting I_{SC} accounting for 26.0 ± 11.5% and 18.6 ± 12.1% of the baseline short-circuit current, respectively (n = 4; P < 0.01). The highest decrease in I_{SC} of 69.2 ± 5.4% after administration of 100 µM Evans blue was observed in H441 shDENAC cells. However, treatment with 300 µM Evans blue did not decreased the I_{SC} further, with the resulting I_{SC} being 67.1 ± 18.3% of the initial baseline level (n = 4; P < 0.01 *vs.* baseline).

Response to apical application of capsazepine

The selective activator of δ-ENaC function, capsazepine, did not increase the I_{SC} in H441 cells, but instead lead to a significant decrease. This effect was observed in the H441 wild-type as well as in the both transfected cell types.

As shown in **Figure 22**, there was a significant drop in the I_{SC} after administration of 20 µM capsazepine. The compound inhibited the currents in H441 wt monolayers by 25.3 ± 15.2% (n = 3; P < 0.05). In H441 shCTRL and H441 shDENAC cells, currents were inhibited by 28.4 ± 6.8% (n = 3; P < 0.01) and 22.4 ± 13.6% (n = 3; P < 0.05), respectively.

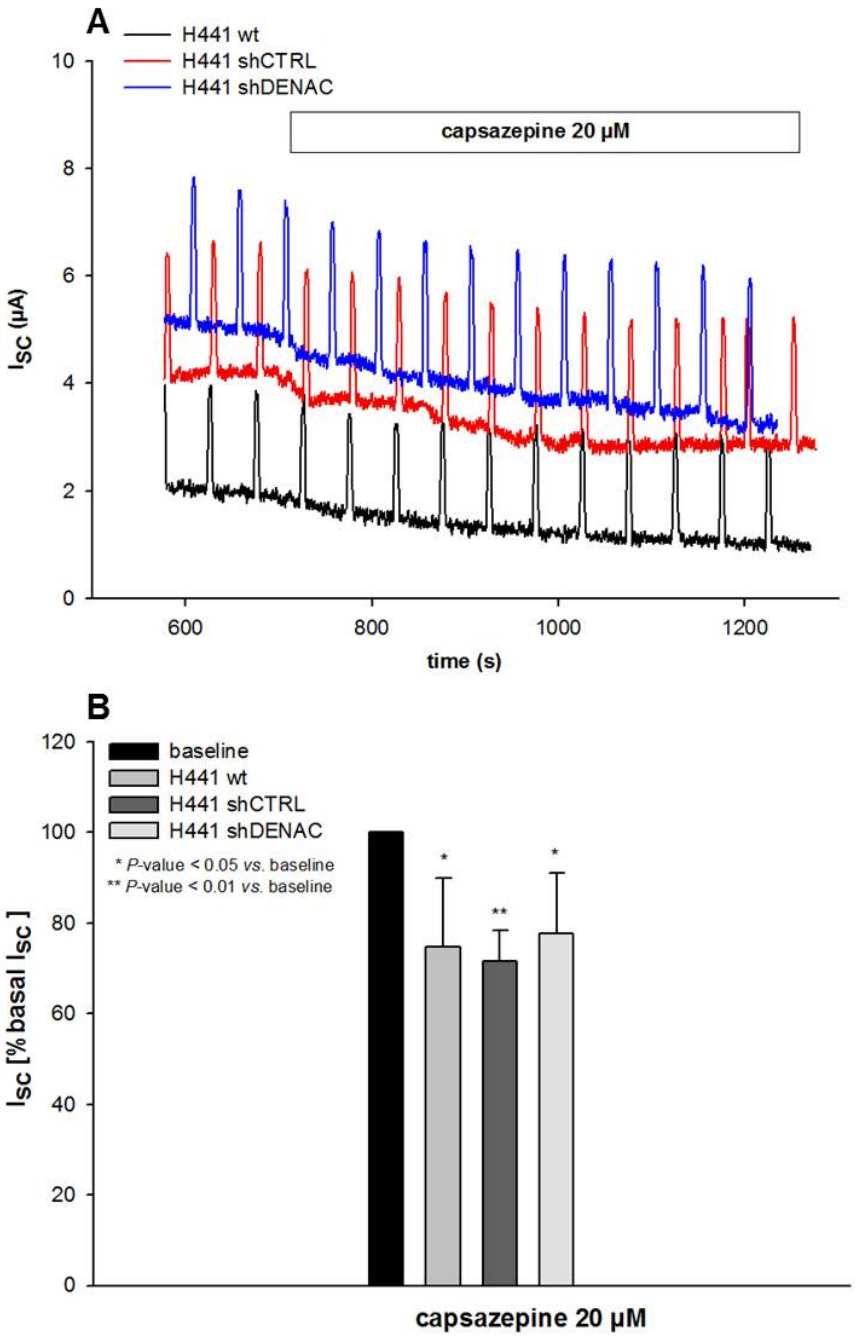

Figure 22

(A) Overlay of the current traces in response to addition of 20 µM capsazepine, obtained during representative Ussing chamber experiments in H441 wild-type (black line), H441 shCTRL (red line) and H441 shDENAC cells (blue line).

(B) Effects of apically administered capsazepine (20 µM) in H441 wt, shCTRL and shDENAC cells. Short-circuit current values were measured 10 min after adding the compound and normalised to the baseline I_{SC} (100%). Results are expressed as means ± SD (n = 3). *, P < 0.05 *vs.* baseline; **, P < 0.01 *vs.* baseline.

Response to apical application of icilin

Despite the fact that icilin was reported to be a selective δ-ENaC activator [58], administration of 60 µM icilin resulted in a significant inhibition of sodium currents in H441 cells (**Figure 23 (B)**).

The I_{SC} of H441 wt decreased to 72.3 ± 16.0% of the initial short-circuit current level (n = 3; P < 0.05). In H441 shCTRL and H441 shDENaC cells, icilin caused a smaller decrease of the I_{SC}, i.e., 11.7 ± 6.0% (n = 3; P < 0.05) and 12.9 ± 4.2% (n = 3; P < 0.01).

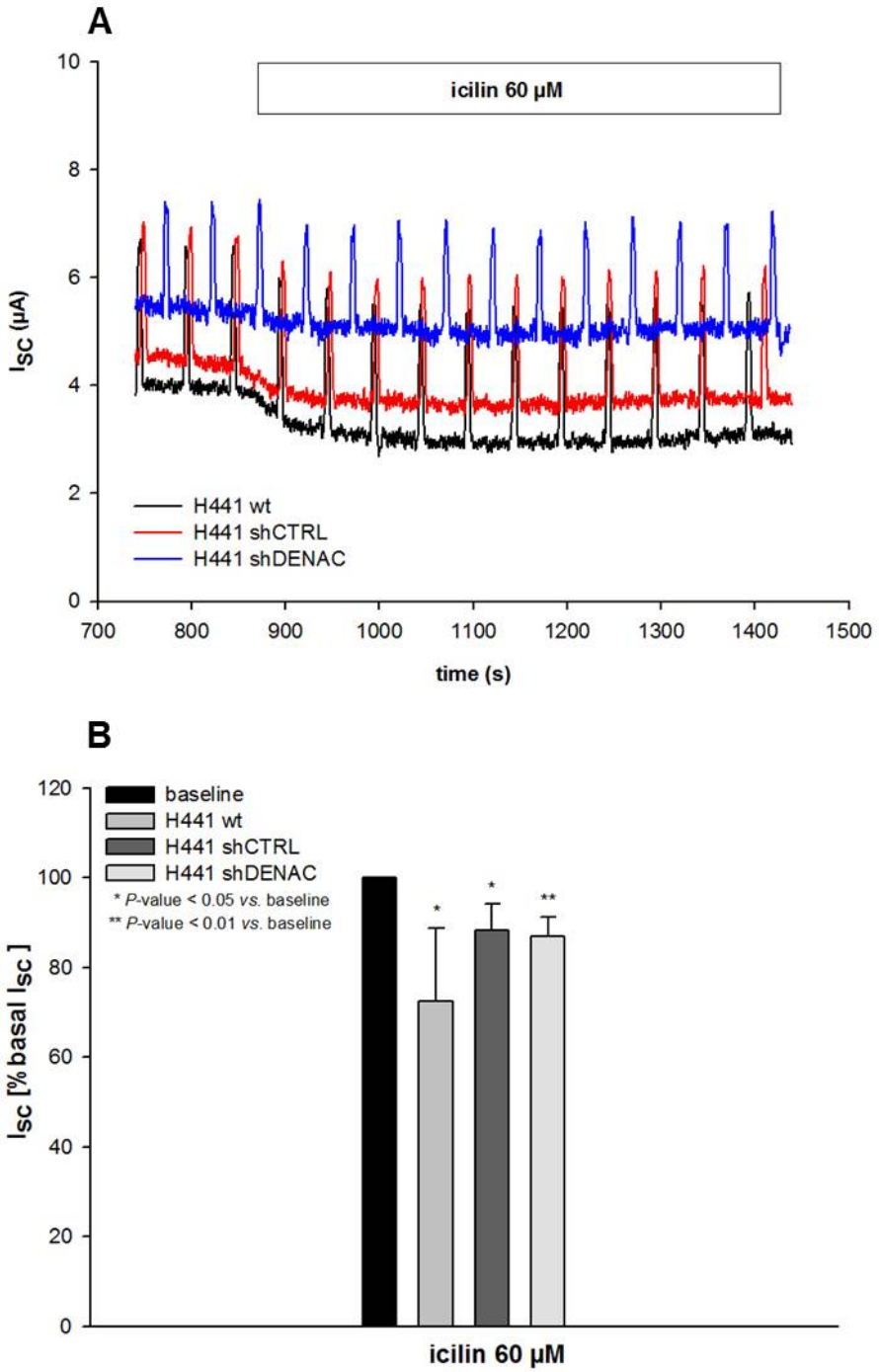

Figure 23

(A) Overlay of the representative current traces obtained in response to 60 µM icilin in H441 wild-type (black line), H441 shCTRL (red line) and H441 shDENAC cells (blue line).

(B) Effects of apically administered icilin (60 µM) in H441 wt, shCTRL and shDENaC cell monolayers. Short-circuit current values were measured 10 min after adding the compound and normalised to the baseline I_{SC} (100%). Results are expressed as means ± SD (n = 3). *, $P < 0.05$ *vs.* baseline; **, $P < 0.01$ *vs.* baseline.

Comparison of the effects exhibited by the alleged modulators of δ-ENaC function in the wild-type cells, mock-transfected as well as in δ-ENaC shRNA transfected H441 cells

Figure 24 compares the effects induced by the administration of Evans blue, capsazepine und icilin in the wild-type (wt) H441 cells to the effects observed in the mock-transfected (shCTRL) and δ-ENaC shRNA transfected (shDENAC) H441 cells.

All compounds tested entailed inhibitory effects in H441 wt, H441 shCTRL and H441 shDENaC cell monolayers, although different outcomes, at least for capsazepine and icilin, were reported by other research groups [47, 54, 58].

On the one hand, only the effects induced by 100 µM Evans blue were significantly different in their amplitude between H441 shDENaC and H441 wt ($P < 0.05$) as well as between H441 shDENaC and H441 shCTRL ($P < 0.01$) cells. However, in contrast to our expectations, the remaining I_{SC} was significantly lower and, therefore, EB-effect was more pronounced in H441 shDENAC monolayers than H441 wt or H441 shCTRL. On the other hand, after application of either 300 µM EB, 20 µM capsazepine or 60 µM icilin, H441 shDENAC cells displayed higher I_{SC} levels compared to H441 wt cells. This suggests that the respective effects were less pronounced in the δ-ENaC shRNA transfected cells. These differences, however, were not significant.

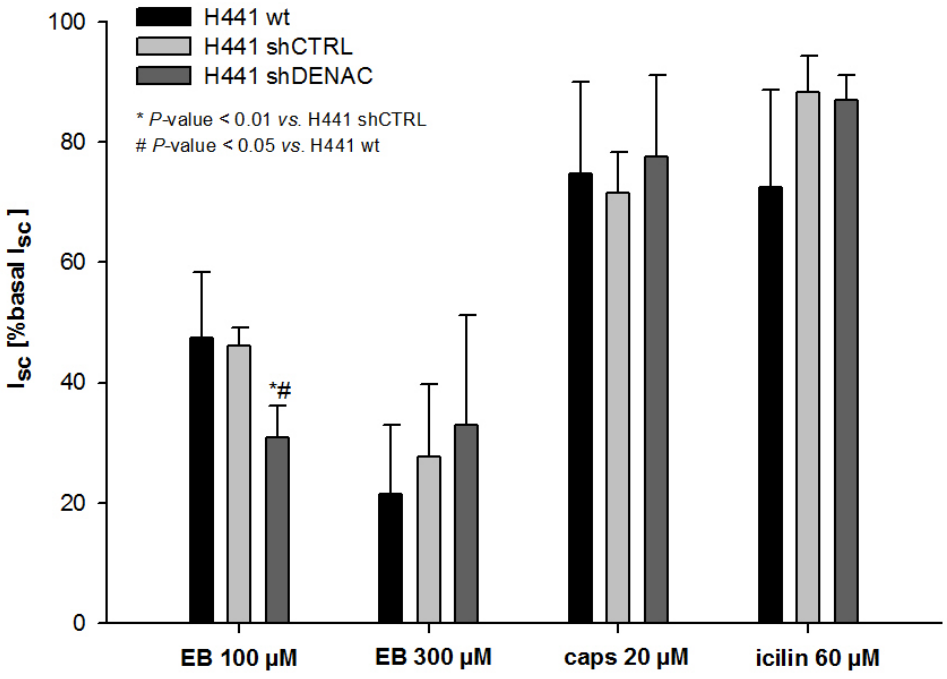

Figure 24

Quantification of responses to 100 µM and 300 µM Evans blue, 20 µM capsazepine and 60 µM icilin in H441 cell monolayers of non-transfected cells (wt) as well as of cells, stably transfected with scrambled shRNA (shCTRL) and shRNA, designed to silence δ-ENaC (shDENAC). Short-circuit currents values, measured after the administration of the relevant compound, were normalised to the basal I_{SC}. Results are expressed as means ± SD (n = 3-4). The statistical significance of the effects versus H441 shCTRL is expressed as *, P < 0.01 and versus H441 wild-type as #, P < 0.05.

Hence, it can be summarised that no significant differences in pharmacological responses to administration of either of the compounds were detected between the wild-type, mock-transfected and δ-ENaC shRNA transfected H441 cells.

3.3 Stable δ-ENaC over-expression in H441 cells

Due to the fact that previous RNAi results proved to be inconclusive a different approach, i.e., δ-ENaC over-expression, was used to investigate the specificity of the observed effects of the δ-ENaC modulators.

3.3.1 Analysis of δ-ENaC over-expression in H441 cells by means of Western blot

Figure 25 shows protein samples from 5 different stably transfected colonies probed with anti-δ-ENaC antibody (DAR) and compared to a negative control sample (n), i.e., lysate of H441 wild-type cells, as well as a positive control sample (p), i.e., lysate of H441 cells transiently transfected with δ-ENaC plasmid. There was no difference between the seven lanes regarding the 100 kDa protein band. However, as shown in **Figure 25**, differences in the band intensities of the 70 kDa band were observed between the lanes. In the negative control sample, only a faint band was detected at 70 kDa, whereas in the positive control a prominent 70 kDa band was present. Only in one of the stably transfected H441 clones (lane 4), a similarly prominent band at 70 kDa was detected. Furthermore, a second band, at around 65 kDa, was observed in sample 4. It can be speculated that this band represents a deglycoslylated form of the full-length δ_1-ENaC protein. As for the other samples (lanes 1-3, 5), they resembled the negative control, with solely a faint band appearing at 70 kDa. Hence, only clone 4 showed stable over-expression of δ-ENaC protein. This clone was expanded, and cells deriving thereof were used for all the subsequent experiments.

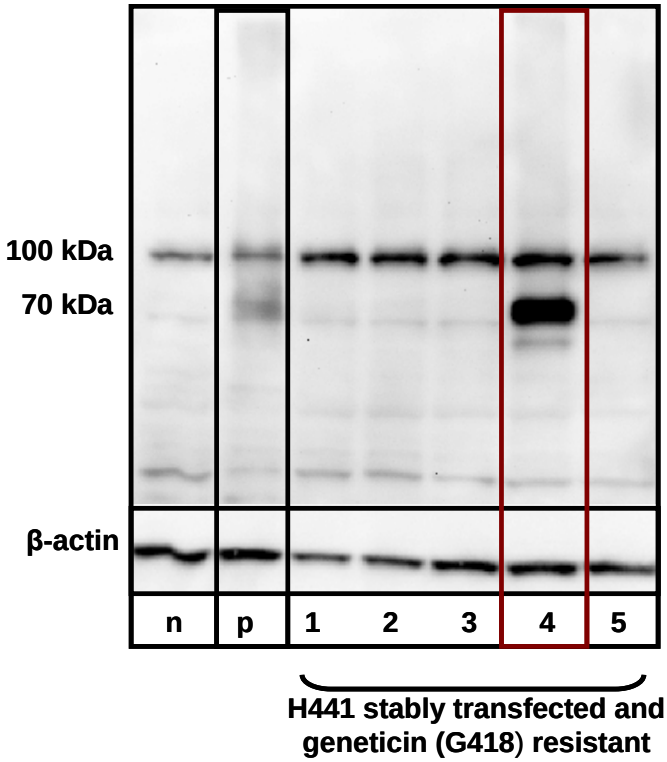

Figure 25

Western blot of δ_1-ENaC protein over-expression. Human bronchiolar H441 cells were transfected with δ_1-ENaC plasmid, integrated into pcDNA3.1(+) vector, and exposed to geneticin for selection. Subsequently, protein was isolated from different geneticin-resistant H441 colonies (Lane 1-5) and analysed by Western blot using anti-δ-ENaC antibody (DAR). n = negative control: wild-type H441 cells. p = positive control: H441 cells transiently transfected with δ_1-ENaC plasmid. Beta-actin was used as loading control.

Further, localisation of the over-expressed δ-ENaC protein was studied. Biotinylation experiments were carried out in order to separate cell surface protein from the intracellularly localised protein. The apical and the basolateral cell membranes were labelled with biotin as described previously. Biotinylated cell surface protein was isolated and analysed by Western blot using anti-δ-ENaC antibody (DAR) (**Figure 26**). Na^+/K^+-ATPase served as a control to test for

potential contamination of the apically biotinylated protein samples with basolateral proteins. In addition, β-actin was used as a control for contamination of the biotinylated membrane protein fractions with intracellular proteins.

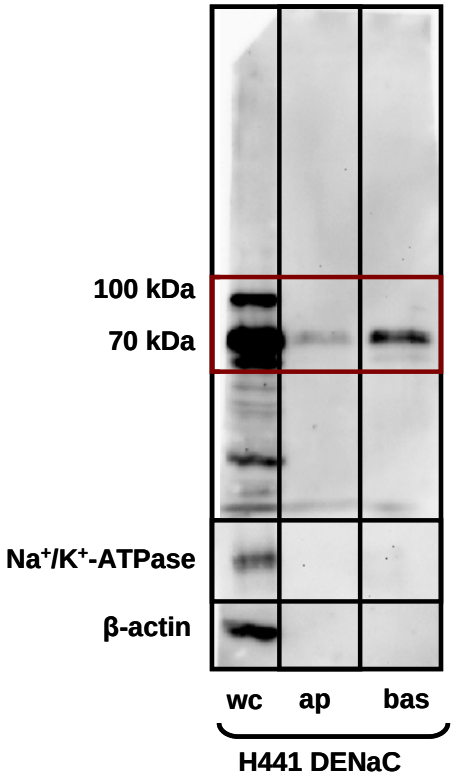

Figure 26

Representative Western blot of whole cell lysate (wc) as well as of apically (ap) and basolaterally (bas) biotinylated surface protein fractions of δ-ENaC over-expressing H441 cells obtained with DAR polyclonal anti-δ-ENaC antibody. Beta-actin and Na+/K+-ATPase were used as controls for potential contamination of the biotinylated samples with intracellular and basolateral protein, respectively.

The first protein lane in **Figure 26** represents the whole cell lysate of the stably transfected, δ-ENaC over-expressing H441 cells. Here, a protein band at 100 kDa as well as two δ-ENaC-specific bands at 70 and 65 kDa were detected using anti-δ-ENaC antibody (DAR). Also, Na^+/K^+-ATPase and β-actin were detected in

the whole cell lysate. In the apically biotinylated sample, a faint band at 70 kDa was detected, however, no band at 65 kDa was observed. In contrast, a distinctive band at 70 kDa and a faint band at 65 kDa were detected in the basolaterally biotinylated sample. Beta-actin was absent from both apical and basolateral samples, indicating that the membrane samples were not contaminated with intracellular contents. Na^+/K^+-ATPase, which is located in the basolateral membrane of epithelial cells, was not detected in either of the biotinylated samples.

Glycosylation of proteins, in particular, O-linked and N-linked addition of glycans to certain amino acids residues, is an important post-translational modification in eukaryotic cells. In order to test whether the distinctive band at 70 kDa represents the glycosylated form of the protein detected at a slightly lower molecular weight (65 kDa), protein sample was treated with PNGase F, a glycoaminidase that cleaves the link between asparagine and N-acetylglucosamine.

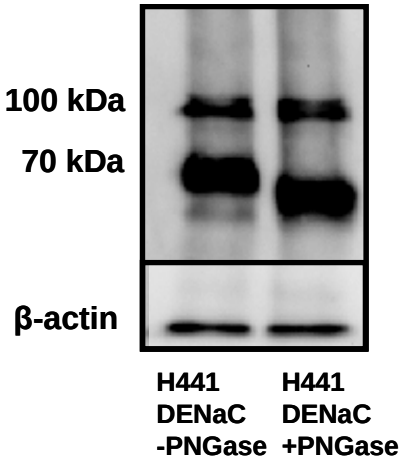

Figure 27

Glycosylation state of δ_1-ENaC, over-expressed in H441 cells. Protein was isolated from δ_1-ENaC over-expressing H441 cells, deglycosylated by treatment with PNGase F and analysed by Western blot using anti-δ-ENaC antibody (DAR). Untreated protein sample was run in parallel. Beta-actin was used as loading control.

Figure 27 shows Western blot analysis of the untreated, negative control sample (labelled H441 DENaC -PNGase) and of a protein sample treated with the deglycosylation enzyme (H441 DENaC + PNGase).

The 100 kDa protein band was present in both samples. However, in the PNGase F treated sample, the 70 kDa band moved slightly downwards to the molecular weight of 65 kDa and, therefore, to the same level as the faint band in the control sample.

3.3.2 Analysis of the localisation of δ-ENaC protein in δ-ENaC over-expressing H441 cells by means of immunofluorescence microscopy

Additionally, immunofluorescence microscopy was carried out to further assess the localisation of δ-ENaC protein in the transfected H441 cells. Localisation of the δ-ENaC protein in H441 wild-type cells was compared to its localisation in

H441 DENaC cells using two different polyclonal anti-δ-ENaC antibodies (SC, DAR). Cell nuclei were counterstained with propidium iodide.

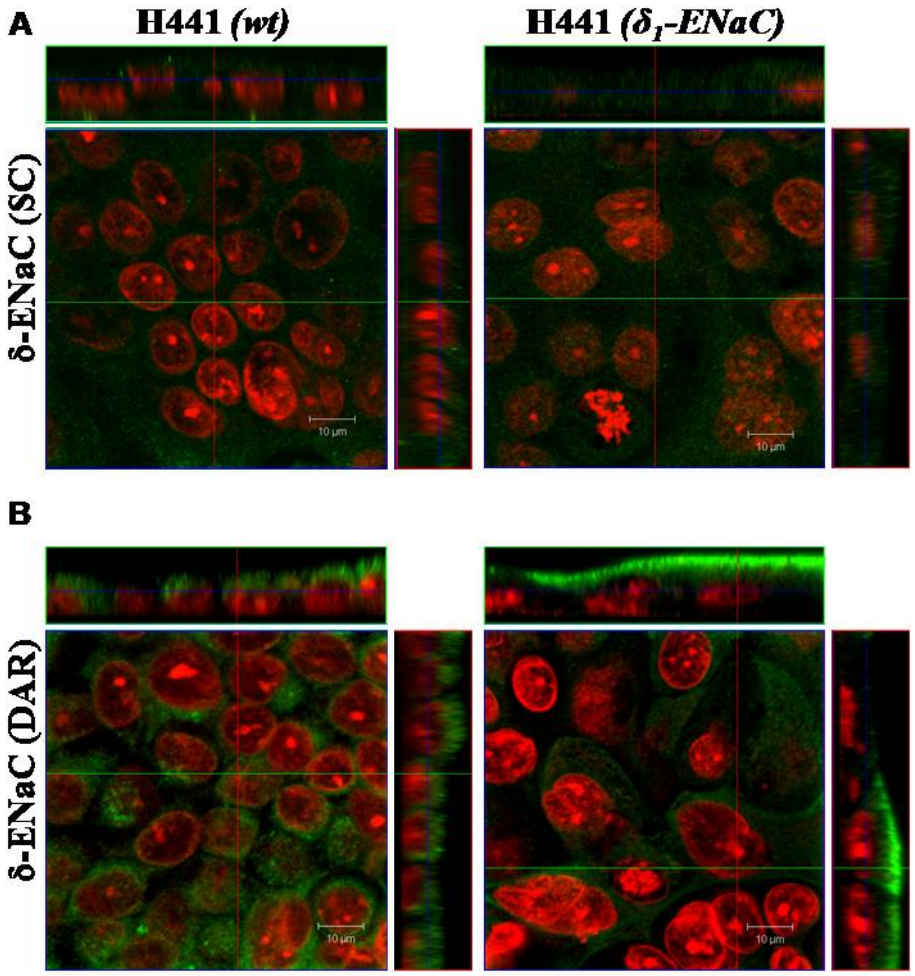

Figure 28

Immunofluorescence microscopy for δ-ENaC (green) in non-transfected (wt) and δ_1-ENaC over-expressing (δ_1-ENaC, green) H441 cells grown on permeable filter inserts and incubated with anti-δ-ENaC SC (A) or DAR (B) antibodies. Cell nuclei were counterstained with propidium iodide (red).

Figure 28 (A) shows confocal laser scanning micrographs of H441 wt and H441 DENaC cells labelled with Santa Cruz anti-δ-ENaC antibody (green). Both cell types display an identical punctuate staining pattern, which is consistent with

predominantly intracellular localisation of δ-ENaC protein. **Figure 28 (B)** shows H441 wt and H441 DENaC cells stained with DAR anti-δ-ENaC antibody (green). In the wild-type H441 cells, again, punctuate staining is observed, however, of higher intensity than with SC antibody. Moreover, the staining is less diffuse. Thus, with clear accumulation of the fluorescent signal around the cell nuclei, it is not possible to state whether the protein is localised intracellularly in compartments, i.e. the endoplasmatic reticulum or the Golgi apparatus, or even expressed in the apical membrane. In the δ_1-ENaC over-expressing cells, the signal localisation is clearly different. The staining appears as a continuous layer above the cell nuclei, suggesting localisation of δ-ENaC protein in the apical cell membrane.

As shown above, the immunostaining obtained with the SC antibody was much less distinct than the signal detected with DAR antibody. Moreover, no difference in the localisation or in the intensity of the fluorescent signal was observed between the wild-type and the transfected H441 cells, when SC antibody was used.

3.3.3 Ussing chamber: Analysis of the δ-ENaC function in δ-ENaC over-expressing H441 cells

As shown in **Figure 29**, H441 wt cells monolayers exceeded TEER values of 400 $\Omega \bullet cm^2$ by day 6 in culture. Delta-ENaC over-expressing cells required approximately 4 days.

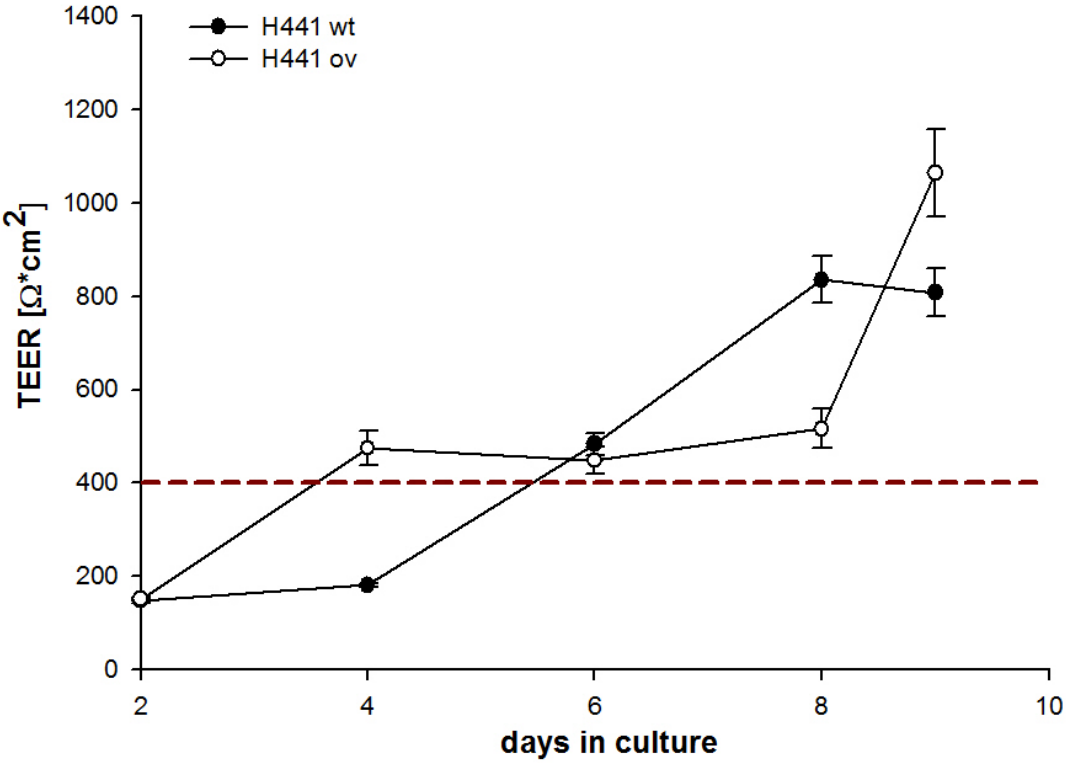

Figure 29

Transepithelial electrical resistance of wild-type H441 (wt, passage 61) and δ-ENaC over-expressing H441 (DENaC, passage p (+11)) cell monolayers grown on permeable filter inserts in course of the time in culture. Red dotted line symbolizes TEER = 400 Ω•cm^2. Results are expressed as means ± SD (*n* = 6).

As shown in **Figure 30**, H441 DENaC cells exhibited significantly higher basal short-circuit current values (8.91 ± 3.06 µA, *n* = 29) than H441 wt cells (4.2 ± 2.1 µA, *n* = 10).

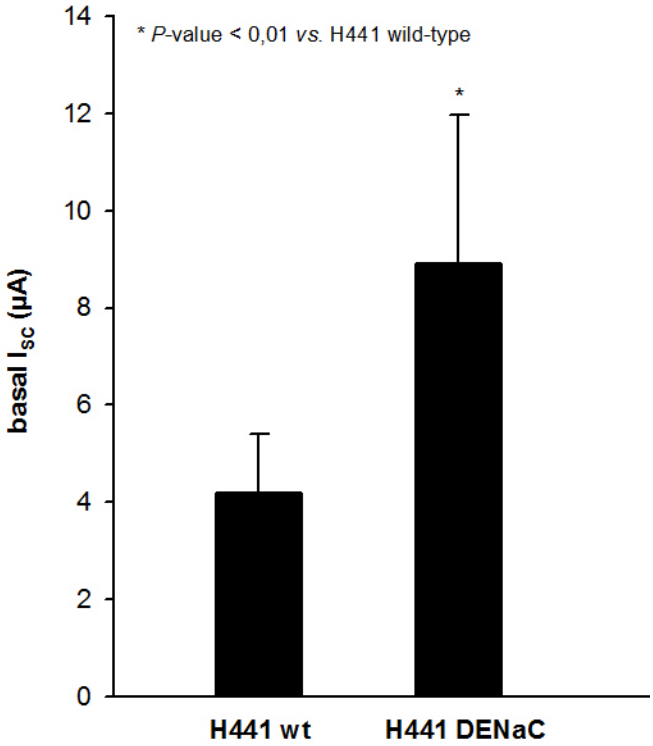

Figure 30

Steady state short-circuit current values (basal I_{SC} [µA]) of H441 wt (*n* = 10) and H441 DENAC (*n* = 29) cell monolayers, obtained under standard conditions (apical and basolateral KRB; pH = 7.4) prior to the start of the measurements. Results are expressed as means ± SD. *, *P* < 0.01 *vs.* H441 wt.

Characterisation of the basal currents in H441 wild-type and H441 DENaC cells

Alpha- and δ-ENaC mediated currents differ in their sensitivity to amiloride. While small concentrations of amiloride, i.e. 10 µM, are sufficient to inhibit α-ENaC mediated currents, ~10-fold concentration is required to block δ-ENaC. To assess the contribution of α-ENaC and δ-ENaC channels to the total sodium currents across the cell monolayers of the wild-type and δ_1-ENaC over-expressing H441

cells, experiments studying the concentration-dependence of current inhibition by amiloride in H441 wt and H441 DENaC cells were conducted.

Figure 31 (A) compares the I_{SC} responses of H441 wt and H441 DENaC cell monolayers to the subsequent application of 10 µM and 100 µM amiloride, respectively. A significant decrease in the I_{SC} of 88.3 ± 5.9% was observed in H441 wt cells after administration of 10 µM amiloride (n = 9; P < 0.01). The I_{SC} was further reduced by 100 µM amiloride to the level of 3.8 ± 4% (n = 9) of the initial current. This additional current decrease was significant (P < 0.01). In contrast, in δ_1-ENaC over-expressing cells, treatment with 10 µM amiloride reduced the I_{SC} by solely 26.3 ± 10.1% (n = 9). Addition of 100 µM amiloride led to a further decrease in the I_{SC}, to the level of 20.3 ± 1.1% of the basal short-circuit current (n = 3). Both effects were significantly different to the basal I_{SC} (P < 0.01).

The major part of the currents in the H441 wt cells were inhibited by 10 µM amiloride, whereas in δ_1-ENaC over-expressing cells these were only about 25%. 100 µM amiloride were required to inhibit the bulk of the currents in H441 DENaC cells. Consequently, the currents across H441 DENaC monolayers were mostly δ-ENaC mediated (insensitive to 10 µM amiloride, however, inhibitable by 100 µM), whilst α-ENaC channels were primarily responsible for current mediation in H441 wt cells.

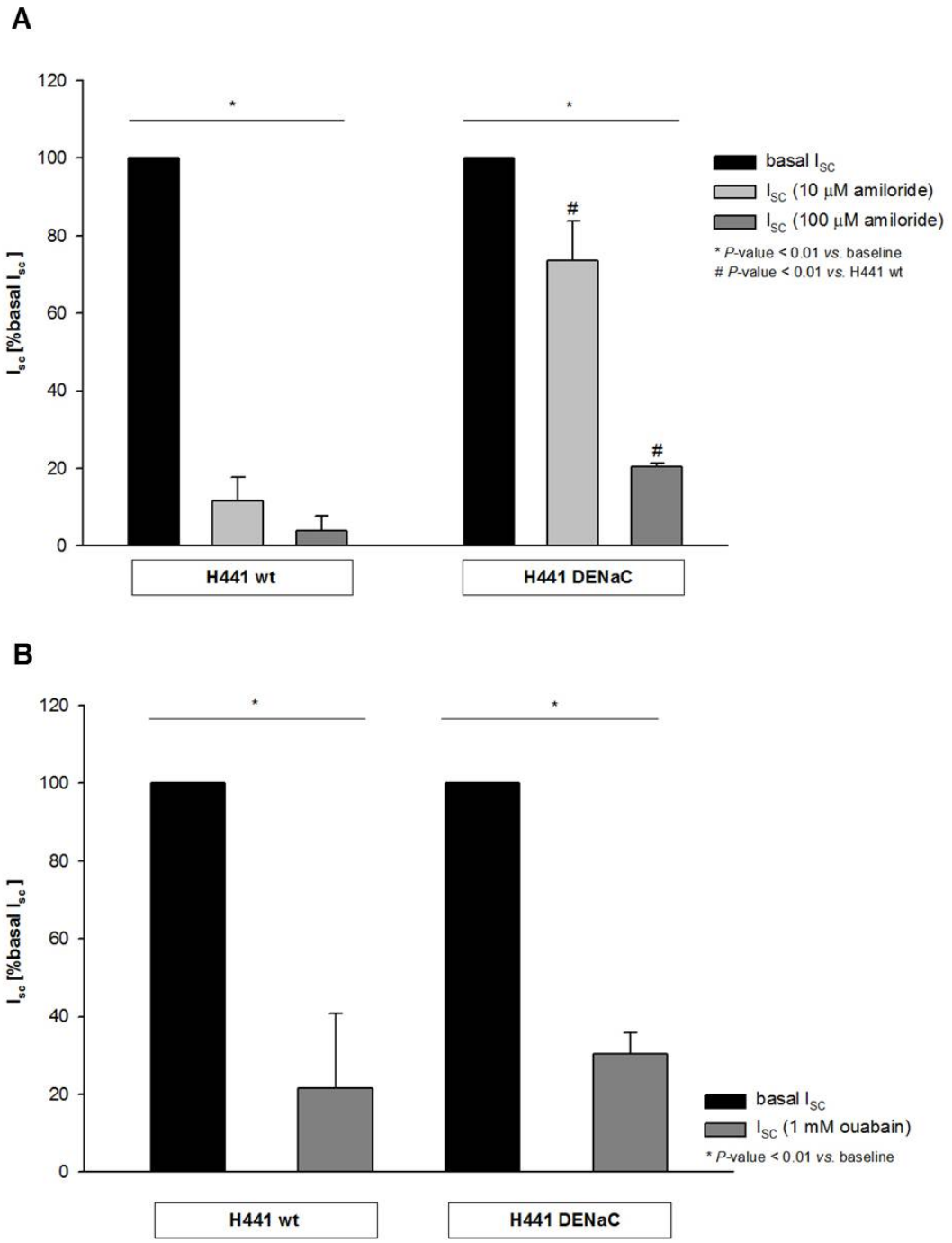

Figure 31

Quantification of responses to the apical application of 10 µM and 100 µM amiloride **(A)** as well as to the basolateral application of 1 mM ouabain **(B)** to the H441 wt and H441 DENaC cell monolayers. Results are expressed as means ± SD (n = 3). The statistical significance of the effects versus baseline is expressed as *, $P < 0.01$; versus the respective effects in the wild-type H441 cells as #, $P < 0.01$;

To exclude the possibility that the observed changes were due to an altered composition of the basal currents, caused by the transfection procedure, the contribution of sodium currents to the overall ion flow was studied in the H441 wt and H441 DENaC cells. To this end, ouabain, an inhibitor of the Na^+/K^+-ATPase, was used.

The basolateral application of 1 mM ouabain led to a significant decrease in the I_{SC} by 78.5 ± 19.4% (n = 5) and by 69.6 ± 5.5% (n = 4) in H441 wt and H441 DENaC, respectively. Both effects were significantly different (P < 0.01) from baseline, however, not from each other **(Figure 31(B))**. This lead to the conclusion that the contribution of sodium currents to the total transepithelial ion transport was similar in H441 wt and H441 DENaC cells and, therefore, unaffected by δ-ENaC over-expression.

Response to apical application of Evans blue, capsazepine and icilin

Delta-ENaC-selective inhibitor Evans blue [47] inhibited short-circuit currents in both wild-type and $δ_1$-ENaC over-expressing H441 cells **(Figure 32 (A)**). The suggested δ-ENaC-selective activator, capsazepine [54], inhibited sodium currents in H441 wt cells. In contrast, the compound had an activating effect on currents in H441 $δ_1$-ENaC over-expressing cells (**Figure 32 (B)**). Icilin, also suggested as a selective δ-ENaC activator [58], increased the I_{SC} of H441 DENaC cell monolayers, as shown in **Figure 32 (C)**, whilst, on the other hand, decreasing the I_{SC} levels in H441 wild-type cells.

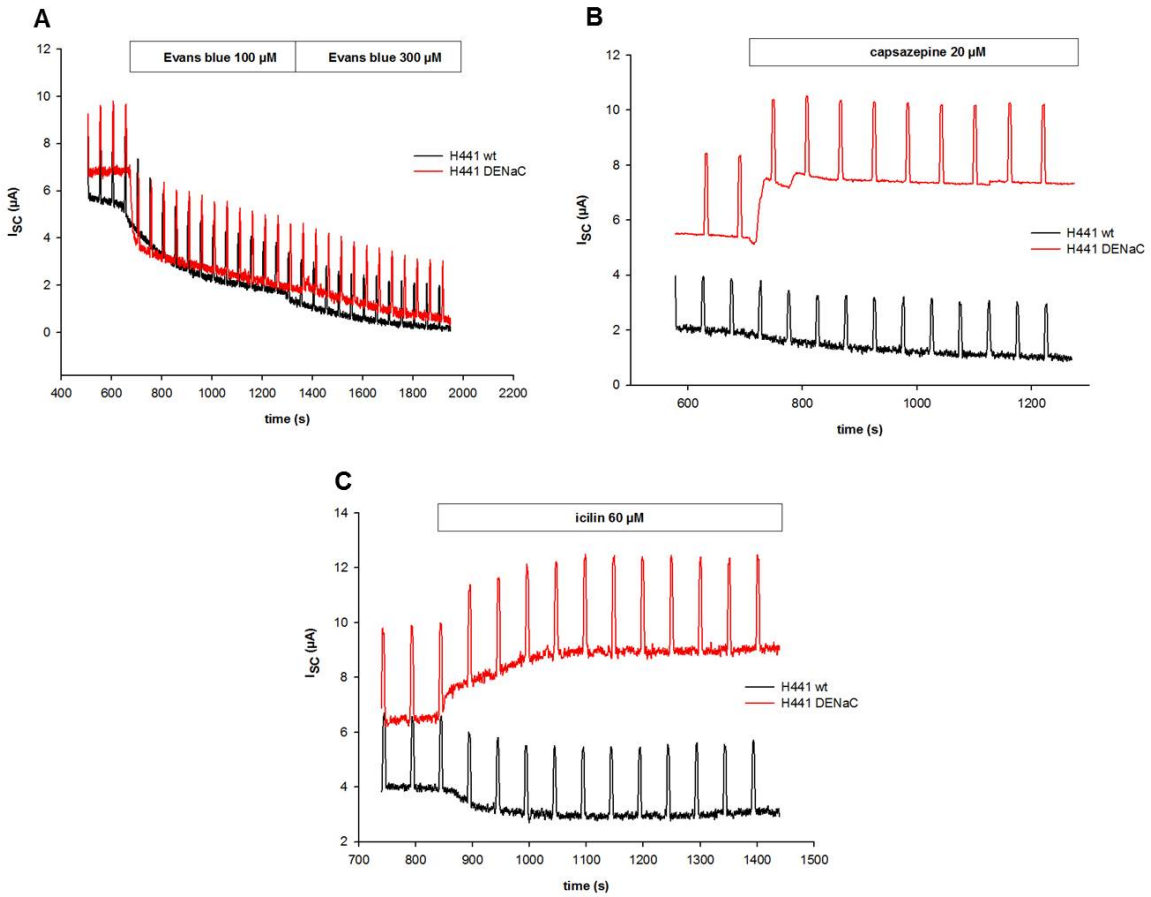

Figure 32

Overlay of the representative current traces obtained in H441 wild-type (black line) and H441 DENAC cells (red line**)** after the administration of 100 µM and 300 µM EB **(A),** 20 µM capsazepine **(B)** and 60 µM icilin **(C)**.

Quantification of effects of the reported δ-ENaC modulators on the short-circuit currents in the wild-type and transfected H441 cells

In order to quantify the pharmacological responses to the respective compounds, the I_{SC}, measured 10 min after the application of the substance, were normalised to the basal I_{SC} (**Figure 33**).

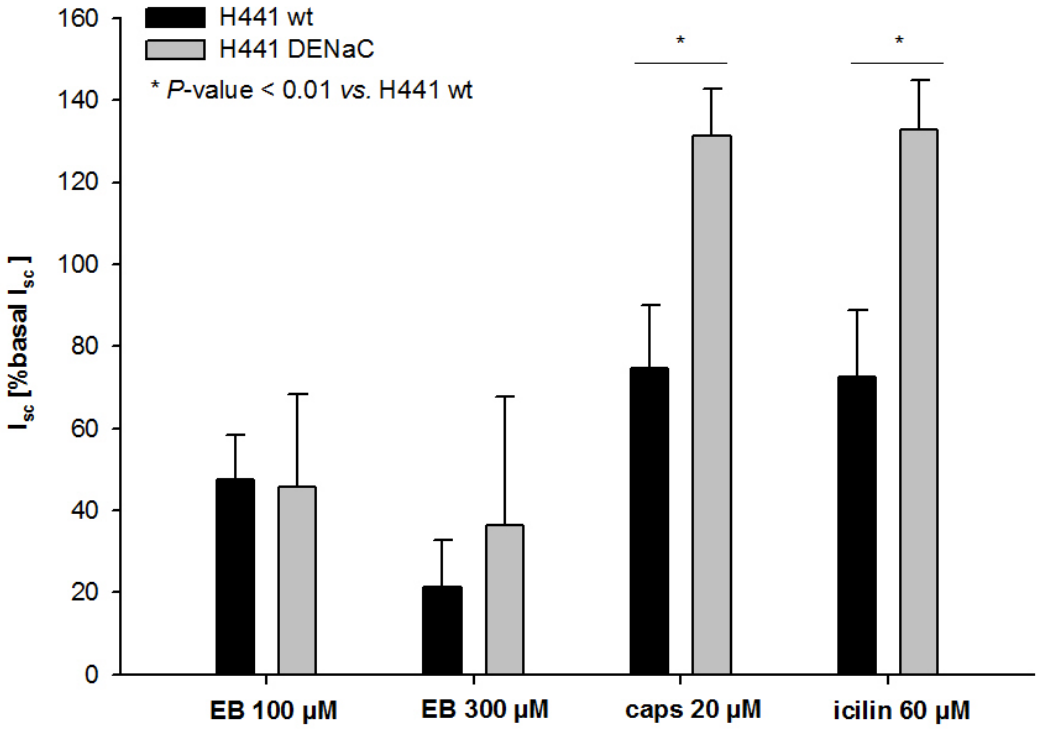

Figure 33

Quantification of the responses to 100 µM and 300 µM Evans blue (EB), 20 µM capsazepine (caps) and 60 µM icilin in H441 wt and H441 DENaC cells. Short-circuit current values were measured 10 min after adding the compound and normalised to the baseline I_{SC} (100%). Results are expressed as means ± SD (n = 3). The statistical significance of the effects versus H441 wt is expressed as *, $P < 0.01$.

Administration of EB 100 µM lead to a decrease in I_{SC} of 54.1 ± 22.5% and 52.6 ± 11.0% in H441 DENaC and H441 wt cells (n = 3), respectively. After adding 300 µM EB to H441 DENaC cell monolayers, a drop in the I_{SC} of 63.5 ± 31.2% (n = 3) was observed. The difference between the effects of 100 µM and 300 µM EB was not significant in H441 DENaC cells. In contrast, in H441 wt cells, 300 µM EB resulted in an inhibition of 78.6 ± 11.5% (n = 3) of the basal I_{SC}, and therefore, a significant additional inhibitory effect compared to 100 µM EB ($P < 0.05$).

However, there was no significant difference between the effects induced by 100 µM and 300 µM EB between H441 DENaC and H441 wt cells, respectively.

Furthermore, **Figure 33** shows that capsazepine led to an increase in I_{SC} of 31.4 ± 11.4% (*n* = 3) in H441 DENaC cells, but to a decrease in I_{SC} of 25.3 ± 15.2% (*n* = 3) in H441 wt cells. The resulting short-circuit currents were significantly different from each other ($P < 0.01$).

Similar was observed in the case of icilin. Administration of 60 µM icilin to H441 DENaC cell monolayers resulted in an increase of I_{SC} of 32.8 ± 12.1% (*n* = 3), as opposed to I_{SC} decrease in H441 wt cells. The effects in both cell types were, hence, significantly different ($P < 0.01$).

Amiloride-sensitivity of the capsazepine- and icilin-evoked currents in δ-ENaC over-expressing H441 cells

In order to test the amiloride-sensitivity of the currents, activated by administration of capsazepine and icilin in δ-ENaC over-expressing H441 cells, the effects observed in the absence and the presence of 10 µM amiloride were studied and compared. After the basal I_{SC} had stabilised, the monolayers were treated with 10 µM amiloride. After about 10 min, the respective compounds, capsazepine or icilin, were applied. The resulting effects reflect the amiloride-insensitive (10 µM) component of the effects observed in the absence of amiloride.

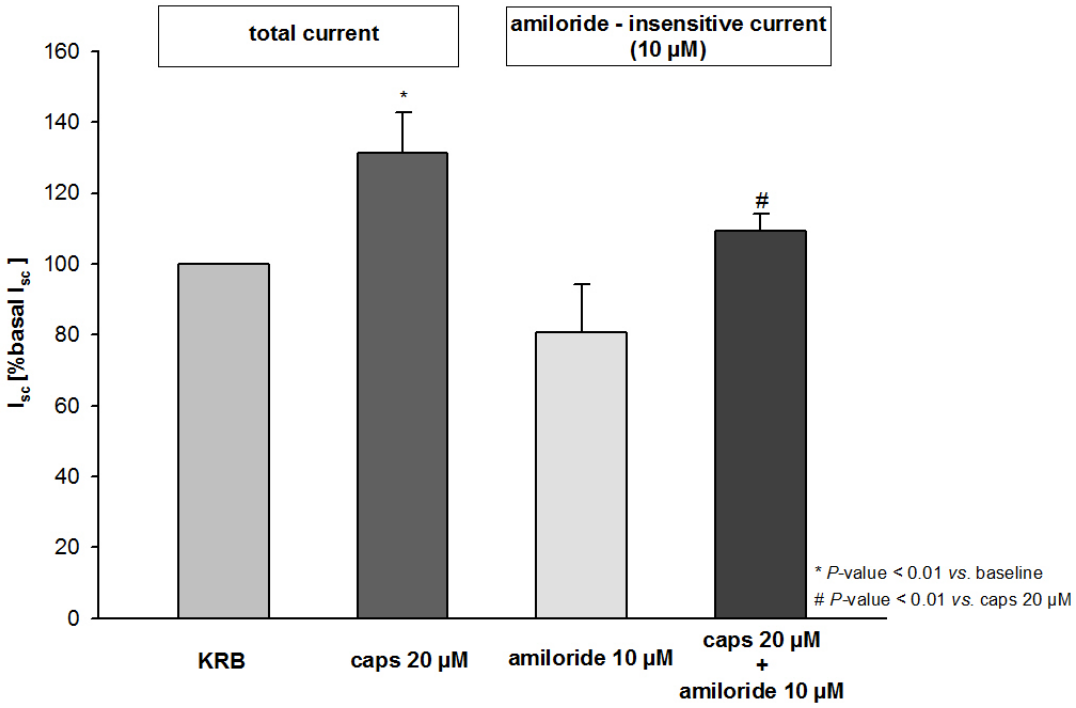

Figure 34

Quantification of the effects on short-ciruit currents in H441 cells, induced by 20 µM capsazepine (caps) in the absence and presence of 10 µM amiloride. Effects in the absence of amiloride represent the total pharmacological response, those in the presence of the amiloride, i.e., the amiloride-insensitive component. Short-circuit current values were measured 10 min after adding the compound and normalised to the baseline I_{SC} (100%). Results are expressed as means ± SD (*n* = 3). The statistical significance of the effects versus baseline is expressed as *, *P* < 0.01; the statistical significance of the effects versus caps 20 µM is expressed as #, *P* < 0.01.

As shown above, capsazepine acted as an activator of the short-circuit currents in δ_1-EnaC over-expressing H441 cells. **Figure 34** demonstrates the significant increase in the total current caused by 20 µM capsazepine (31.4 ± 11.4%, *n* = 3, *P* < 0.01). Treatment of H441 DENaC cell monolayers with 10 µM amiloride reduced the I_{SC} by 19.2 ± 13.6% (*n* = 3) of the basal level. Due to a rather high standard deviation, the effect was not significant. Administration of 20 µM

capsazepine to amiloride-treated H441 DENaC monolayers lead to an increase in the I_{SC} of 28.5 ± 4.8% (*n* = 3), compared to the I_{SC} in the presence of amiloride. Thus, the extent of activation was similar for both, the total and the amiloride-insensitive currents, suggesting that stimulation of currents insensitive to 10 µM amiloride accounted for the increase in total currents.

Alpha- and δ-ENaC mediated currents differ in their sensitivity to amiloride. While small concentrations of amiloride, i.e., 10 µM, are sufficient to inhibit α-ENaC mediated currents, ~10-fold concentration is required to block δ-ENaC. Hence, the described observations suggest that capsazepine-induced currents were mediated by δ-ENaC, rather than by α-ENaC-containing channels.

Icilin as an activator of δ-ENaC function, significantly increased the total currents of H441 DENaC by 32.8 ± 12% of basal I_{SC} (*n* = 3, *P* < 0.01), as shown in **Figure 35**. When added in the presence of 10 µM amiloride, icilin led to an increase of 39.2 ± 2.7% of the amiloride-insensitive I_{SC} (*n* = 3, *P* < 0.01). As in the case of capsazepine, it can be concluded that the icilin-induced increase in total current was mostly due to stimulation of currents insensitive to 10 µM amiloride. Therefore, stimulated currents were likely to be mediated by δ-ENaC, rather than by α-ENaC.

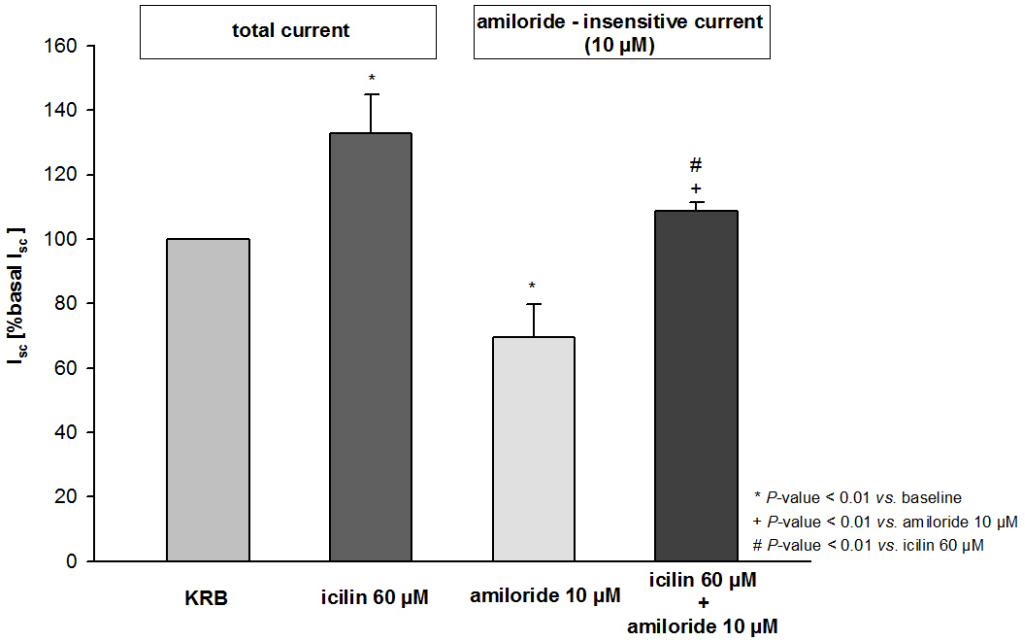

Figure 35

Quantification of the effects on short-ciruit currents in H441 cells, induced by 60 µM icilin in the absence and presence of 10 µM amiloride. Effects in the absence of amiloride represent the total pharmacological response, those in the presence of the amiloride, i.e., the amiloride-insensitive component. Short-circuit current values were measured 10 min after adding the compound and normalised to the baseline I_{SC} (100%). Results are expressed as means ± SD (*n* = 3). The statistical significance of the effects versus baseline is expressed as *, *P* < 0.01; versus 60 µM icilin as #, *P* < 0.01; versus 10 µM amiloride as +, *P* < 0.01.

3.3.4 Patch-clamp experiments

Transepithelial measurements in modified Ussing chambers allow to investigate the effects of pharmacological modulators, e.g., channel activators or blockers, on the ion transport across confluent cell monolayers. Patch-clamp technique, on the other hand, facilitates to study the ion transport across the membrane of a single cell (whole-cell mode) or even via a single channel (single channel mode). To confirm the findings obtained with δ-ENaC modulators in Ussing chamber

studies, patch-clamp experiments were carried out using H441 DENaC cells (passage (+8) - (+12)). Only isolatedly growing cells were used in these studies. All experiments were conducted in the whole-cell mode.

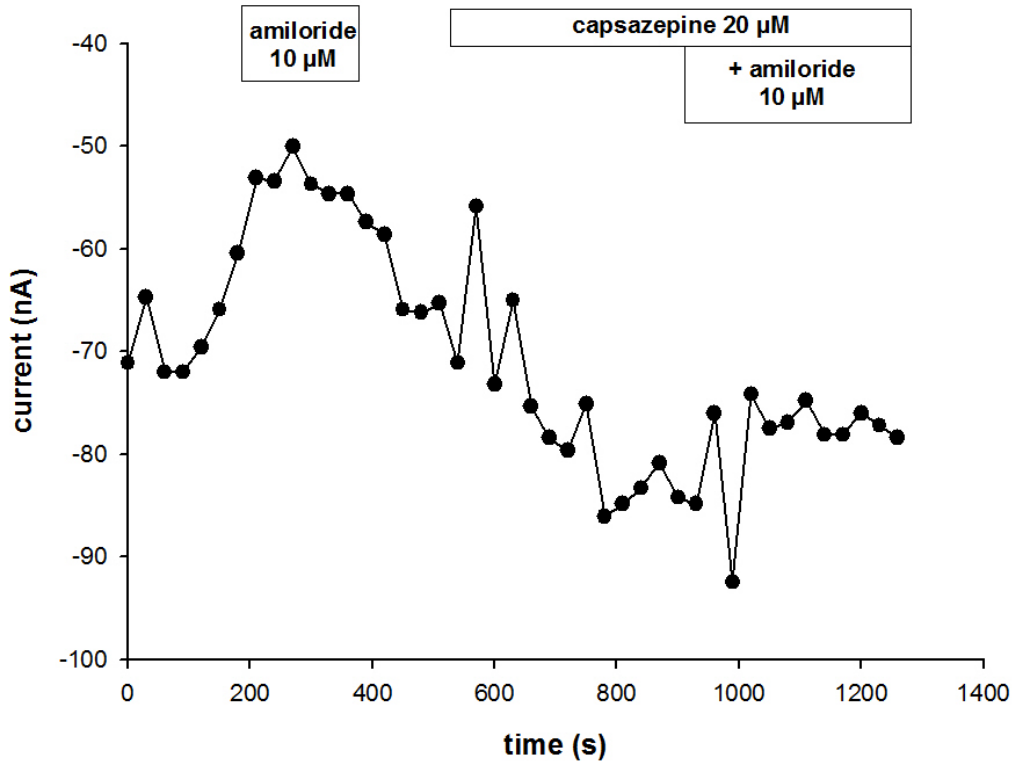

Figure 36

Representative whole-cell current trace from a H441 DENaC cell recorded at the holding potential of -60mV.

Membrane currents of cations are negative when ions move inward, as shown in **Figure 36,** a representative whole-cell current trace recorded in a H441 DENaC cell. The slight positive shift in the current from -70nA to -50nA, after the application of 10 µM amiloride, underlines that the recorded traces are inhibited by amiloride. Capsazepine as an activator, on the other side, results in a more negative current (-90nA) then the initial value caused by the bigger inward flux of

sodium ions. The agonistic impact of capsazepine is partially abolished by a reapplication of amiloride.

Figure 37 shows the quantification of the observed effects. 25.8 ± 7.0% (*n* = 3) of the sodium currents were inhibited by amiloride in H441 DENaC cells, whereas capsazepine activated currents by 40.9 ± 15.0% (*n* = 3) (*P* < 0.01). In capsazepine-treated cells, 20.4 ± 11.7% of the measured current were amiloride-sensitive.

These data confirm that capsazepine activated sodium currents in δ-ENaC over-expressing cells. The stimulation of the ion transport occurred not only across the intact, confluent cell monolayer (Ussing chamber) but also on the single cell level (patch-clamp). Moreover, this stimulation was mostly due to activation of currents insensitive to 10 µM amiloride (**Figure 37**) and, therefore, not α-ENaC mediated. This is consistent with our previous findings in the Ussing chamber experiments (**Figure 34**).

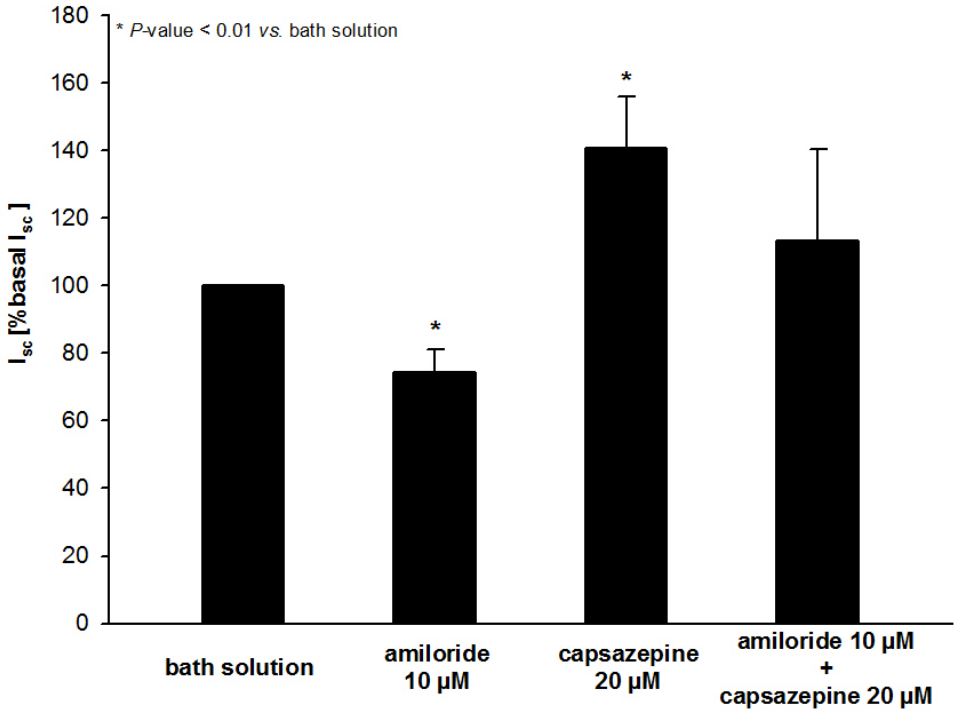

Figure 37

Effects of amiloride and capsazepine on the sodium currents in H441 DENaC cells, measured by patch-clamp technique in the whole-cell configuration. Results are expressed as means ± SD (n = 3). The statistical significance of the effects versus currents measured in the bath solution is expressed as *, $P < 0.01$.

4 DISCUSSION

The aim in this thesis was to investigate the expression, cellular localisation and function of δ-ENaC in human respiratory epithelial cells as well as to determine the δ-ENaC specificity of the modulators' effects observed in H441 and Calu-3 cells.

The Western blot and IFM data imply that δ-ENaC is in fact expressed in H441 and Calu-3 wild-type cells on protein level, confirming previous publications by other groups that state the expression of δ-ENaC in H441 cells [20] and human nasal epithelium [21]. However, results of cell surface protein biotinylation suggest that it is not or only marginally expressed in the cell membranes.

RNAi experiments aiming to silence the expression of δ-ENaC protein were performed, but failed to show significantly less pronounced band intensities in shRNA transfected cells. The reason for this seemingly unsuccessful attempt of down-regulating the δ-ENaC expression might lie in an already rather low expression level of δ-ENaC in H441 and Calu-3 wt cells. Therefore, further down-regulation does not show a difference in expression levels.

An alternative approach for investigating the expression and localisation was the over-expression of δ-ENaC protein in H441 cells. To this end, cells were transfected with δ_1-ENaC plasmid. The immunoblots of the biotinylated samples demonstrated the presence of δ-ENaC protein in both apical and basolateral membranes. Interestingly, higher amounts of δ_1-ENaC protein were observed in the basolaterally biotinylated samples. This was rather unexpected since ENaC channels are usually localised in the apical membranes [1, 2]. Furthermore, Na^+/K^+-ATPase, as a basolateral marker, was not detected in either of the biotinylated samples, which leads to the conclusion, that the biotinylated cell

lysates might have been deficient. Deglycosylation of cell lysates with PNGase F indicates that the 65 kDa band, which also appears in the H441 DENaC whole-cell immunoblots, represents the non-glycosylated δ_1-ENaC protein.

Immunofluorescence microscopy demonstrated that the over-expressed δ_1-ENaC protein is localised in the apical membrane of H441 DENaC cells. Compared to IFM images of H441 wt cells there is a distinct difference in the localisation pattern, adding to our thesis that in wild-type cells δ-ENaC is not expressed in the apical membrane but rather intracellular or in certain cellular compartments.

Ji e*t al.* reported evidence of δ-ENaC expression in H441 and A549 cells on mRNA level and protein level. They, however, did not provide functional data in these organotypic cell models but instead used heterologous expression systems for patch-clamp experiments [20].

To underline our assumption with functional data, Ussing chamber measurements were carried out with wild-type, δ-ENaC mock-transfected and down-regulated cells (H441, Calu-3) as well as with δ-ENaC over-expressing cells (H441). Each compound had a significant impact on the short-circuit currents in the wild-type and the transfected cells, adding to the assumption that a low membrane abundance could not be down-regulated further or rather does not result in an observably different effect of the channel's function.

Moreover, the studies conducted in our lab have shown that the three compounds suggested as selective δ-ENaC modulators had a different impact on the short-circuit currents in H441 and Calu-3 wild-type and RNAi transfected cells than the effects reported by other research groups in heterologous expression systems [47, 54, 58] and native tissue [21].

In contrast to our previous experiments with H441 wt cells, in which currents were inhibited by capsazepine and icilin, currents in δ_1-ENaC over-expressing H441 monolayers were activated by capsazepine and icilin. Evans blue exhibited inhibitory effects on the short-circuit currents in both cell types.

Taking the results of δ-ENaC over-expression into account, it can be concluded that the responses in H441 wt as well as in Calu-3 wt monolayers were not δ-ENaC specific. Hence, like in H441 cells, δ-ENaC protein, albeit being present according to Western blot results, does not play a functional role in Calu-3 and H441 wild-type cells due to low membrane abundance.

To determine the contribution of α-ENaC and δ-ENaC channels to the total sodium currents in H441 wt and H441 DENaC cells, experiments studying the concentration dependence of the current inhibition by amiloride were conducted. While α-ENaC currents are inhibited by small concentrations of amiloride (10μM), ~10-fold concentration is required to block δ-ENaC. Regarding H441 wt cells, the major part of the current was blocked by the administration of 10 μM amiloride, which lead to the conclusion that currents in H441 wild-type cells are mainly mediated by α-ENaC and αβγ-ENaC channels. In contrast, the responses in H441 DENaC cells were significantly different, with the major portion of the current being insensitive to 10 μM, however, inhibitable by 100 μM amiloride.

Subsequently, to confirm that the pharmacological responses, observed in H441 DENaC cells, mainly originated from the interactions of the respective compounds with δ_1-ENaC channels, the amiloride-sensitivity of the induced currents was tested. Although H441 DENaC monolayers were pre-treated with 10 μM amiloride and, hence, α-ENaC channels were inhibited, both capsazepine and icilin were still able to stimulate currents. These results confirm that the

current activation caused by capsazepine and icilin was due to activation of δ_1-ENaC channels. Patch-clamp studies in whole-cell modification underlined the stimulatory effect of capsazepine on the sodium currents in δ-ENaC over-expressing H441 cells. Moreover, the effects were shown to be insensitive to 10 µM amiloride and, therefore, mediated by δ- rather than by α-ENaC channels.

Although Ussing chamber experiments, using H441 wt cell monolayers in standard KRB and sodium-free buffer, suggest that the pharmacological responses to δ-ENaC modulators were sodium-dependent, the responses to the individual compounds, we observed in organotypic and δ-ENaC down-regulated cell models, were not in accordance with those described in heterologous expression systems. All three substances are known to interact with proteins other than δ-ENaC. Evans blue is said to activate large-conductance Ca^{2+}-activated K^+ channels [60, 61]. Capsazepine is a competitive antagonist of TRPV1 [48, 49, 50]; furthermore, it blocks voltage-dependent calcium and potassium channels [51, 52]. Icilin works as an agonist for the transient receptor potential melastatin subfamily 8 and ankyrin-like subfamily 1 [55, 56, 57, 62]. Contrary to others, we are assuming that the compounds' effects, observed in our hands, most likely originated from modulation of other targets and that the compounds are not necessarily δ-ENaC specific. The reason that the effects observed in δ-ENaC over-expressing H441 cells match the effects observed by Yamamura and others [47, 54, 58], but are different from effects recorded in organotypic cell models, might be caused by effects, mediated by δ-ENaC channels, that are overlaying the effects mediated by the other targets. Furthermore, the affinity of the respective compounds to δ-ENaC might be higher than the affinity to other targets. Moreover, it might be the case that not all of the

above-mentioned targets are present in *X. laevis* oocytes. Additionally, Bangel-Ruland draws a conclusion on the δ-ENaC specificity by using only one δ-ENaC modulator [21]. Therefore, the usage of these compounds as tools for characterisation of δ-ENaC function in native cells is rather limited.

In conclusion, we found that the δ-ENaC subunit is expressed in H441 and Calu-3 cells on protein level, although it does not seem to play a physiological role in respiratory epithelial cells due to low membrane abundance. However, in order to further study the functional expression as well as the physiological role of δ-ENaC in the lung epithelium, but also in other tissues, additional investigations aiming to identify specific δ-ENaC modulators are needed.

5 SUMMARY

The epithelial sodium channel (ENaC) is an amiloride-sensitive, non-voltage gated ion channel, which is widely distributed throughout epithelial as well as non-epithelial tissues. Alpha-, β- and γ-subunits are predominantly found in epithelial tissues, i.e., in the lung and kidney. In the lung, αβγ-ENaC plays a crucial role at birth, when the lung changes from the liquid-filled to the air-filled state. In addition, δ-ENaC subunit mRNA and protein are present in the human lung tissue, raising the question about the physiological role of δ-ENaC in this organ. A number of xenobiotics have been suggested to be selective δ-ENaC modulators, i.e., Evans blue (inhibitor) as well as capsazepine and icilin (activators). In this study, our aim was to investigate the expression, cellular localisation and function of δ-ENaC in human respiratory epithelial cells. Furthermore, we assessed the specificity of the mentioned δ-ENaC modulators.

First, we studied the sodium-dependence of the alleged activators' and inhibitors' effects in H441 cells. To this end, Ussing chamber experiments were carried out in Krebs-Ringer-Buffer (KRB) and in sodium-free KRB. In contrast to previously published studies, all of the above mentioned compounds displayed inhibitory effects in H441 cells in KRB. In sodium-free buffer, however, none of the substances led to significant changes in I_{SC}, indicating a sodium-dependence of the observed effects.

Since the compounds' effects in our hands were different from the previous observations by others, we tested the δ-ENaC specificity of the effects by silencing (H441 and Calu-3) as well as over-expressing (H441) δ-ENaC. First, the

effects of the stable knock-down of the δ-ENaC protein in H441 and Calu-3 cells were assessed on the protein level by Western blot analysis. Moreover, the effects of δ-ENaC modulators on the currents in transfected, mock-transfected and non-transfected cells were compared. However, no significant reduction was detected in protein abundance and in the modulators' effects in the δ-ENaC knockdown-transfectants, suggesting that the attempt to down-regulate the expression and function of δ-ENaC was not successful.

The over-expression of δ-ENaC in H441 cells was also assessed by Western blot and Ussing chamber experiments. Furthermore, immunofluorescence microscopy (IFM) and patch-clamp studies were carried out. After the transfection with δ_1-ENaC plasmid, H441 clones stably over-expressing δ-ENaC protein, as confirmed by Western blot, were selected, expanded and used for subsequent analysis. IFM revealed the localisation of the over-expressed δ-ENaC channels in the apical cell membrane. In contrast to the effects in the wild-type H441 cells, currents in δ_1-ENaC over-expressing H441 monolayers were activated by capsazepine and icilin. Evans blue exhibited inhibitory effects on the short-circuit currents in both cell types. Patch-clamp studies confirmed that the current activation caused by capsazepine was due to activation of δ_1-ENaC channels.

Collectively, our observations revealed that the compounds' effects in the organotypic cell models likely originated from modulation of other, yet unknown, targets different from δ-ENaC. Thus, under the chosen, unstimulated conditions, δ-ENaC did not contribute to the transepithelial sodium transport across the respiratory epithelium. In addition, the reported δ-ENaC modulators were proven to be of a limited suitability for use in organotypic cell models. Therefore, the identification of more and more specific δ-ENaC modulators is required in order

to study the functional expression as well as the physiological role of δ-ENaC in the lung epithelium and other tissues.

6 ZUSAMMENFASSUNG

Amilorid-sensitive und spannungsunabhängige epitheliale Natriumkanäle (ENaC) sind sowohl in epithelialem als auch in nicht-epithelialem Gewebe weit verbreitet; wobei α-, β- und γ-Untereinheiten überwiegend in epithelialem Gewebe, z.B. der Lunge und der Niere, vorkommen. Im Respirationstrakt spielt αβγ-ENaC eine entscheidende Rolle während der Geburt, wenn die Lunge von einem mit Flüssigkeit gefüllten zu einem Luft-gefüllten Organ wird. Delta-ENaC mRNA und Protein sind in der menschlichen Lunge ebenfalls vorhanden. Daraus ergibt sich die Frage nach der physiologische Funktion δ-ENaCs im Lungenepithel. Als spezifische δ-ENaC Modulatoren wurden Evans blue (Antagonist) sowie Capsazepin und Icilin (Agonisten) in der Literatur genannt. Unser Ziel war, die Expression, Lokalisation und Funktion von δ-ENaC in Epithelzellen des menschlichen Respirationstraktes genauer zu untersuchen, sowie in weiterer Folge die Spezifität der δ-ENaC Modulatoren zu beurteilen.

Als Erstes wurde die Natriumabhängigkeit der, durch die mutmaßlichen Agonisten und Antagonisten, hervorgerufenen Effekte in H441 Zellen untersucht. Hierzu wurden Ussingkammerstudien sowohl in Krebs-Ringer-Puffer (KRP) als auch in Natrium-freien KRP ausgeführt. Es konnte eine definitive Natriumabhängigkeit der beobachteten Effekte festgestellt werden, da keine der Verbindungen zu einer signifikanten Änderung der I_{SC} in Natrium-freiem KRP führte. In regulärem KRP hingegen wurde bei allen Substanzen eine inhibierende Wirkung festgestellt.

Da die von uns beobachteten Effekte von denen in vorherigen Publikationen abwichen, haben wir versucht die δ-ENaC Spezifität der verwendeten Substanzen durch δ-ENaC Herabregulierung (H441 und Calu-3) und durch Überexpression (H441) genauer zu eruieren.

Die stabile Herabregulierung des δ-ENaC Proteins in H441 und Calu-3 Zellen wurde anhand von Western blot Analysen beurteilt. Danach wurden die Effekte der δ-ENaC Modulatoren auf die Elektrophysiologie transfizierter Zellen mit den Effekten auf Kontroll-transfizierten und nicht-transfizierten Zellen verglichen. Da weder bei der Proteinmenge noch bei den modulatorischen Effekten eine signifikante Abnahme zu erkennen war, kann von einer erfolglosen Herabregulierung der δ-ENaC Expression ausgegangen werden.

In weiterer Folge wurde die stabile Überexpression von δ-ENaC durchgeführt. Nach der Transfektion der H441 Zellen mit dem δ_1-ENaC Plasmid, wurden die überexprimierenden Klone mittels Western blot Analyse bestimmt und danach vermehrt. Anhand der Immunofluoreszenzmikroskopie konnten die δ-ENaC Kanäle in der apikalen Zellmembran lokalisiert werden. Im Gegensatz zu den Wildtyp Zellen wurden die Kanäle in δ-ENaC überexprimierenden Zellen durch Capsazepin und Icilin aktiviert und durch Evans blue inhibiert. Patch-clamp Experimente festigten die Annahme, dass die aktivierende Wirkung von Capsazepin durch δ_1-ENaC vermittelt wurde.

Diese Ergebnisse führen zu dem Schluss, dass unsere Beobachtungen in organotypischen Zellmodellen wahrscheinlich auf der Modulation anderer Zielstrukturen basieren. Da sich die Modulatoren somit als nur bedingt δ-ENaC spezifisch herausstellten, ist die Ermittlung weiterer, δ-ENaC spezifischerer

Verbindungen dringend notwendig, um sowohl die Expression als auch die physiologische Funktion von δ-ENaC zu untersuchen.

7 REFERENCES

(1) ALVAREZ DE LA ROSA D, CANESSA CM, FYFE GK & ZHANG P. (2000). Structure and Regulation of amiloride-sensitive sodium channels. *Annu Rev Physiol* **62,** 573-594.

(2) KELLENBERGER S & SCHILD L. (2002). Epithelial sodium channel/degenerin family of ion channels: a variety of functions for a shared structure. *Physiol Rev* **82,** 735-767.

(3) CANESSA CM, HORISBERGER JD & ROSSIER BC. (1993). Epithelial sodium channel related to proteins involved in neurodegeneration. *Nature* **361,** 467-470

(4) CANESSA CM, SCHILD L, BUELL G, THORENS B, GAUTSCHI I, HORISBERGER JD & ROSSIER BC. (1994b). Amiloride-sensitive epithelial Na_+ channel is made of three homologous subunits. *Nature* **367,** 463-467.

(5) RENARD S, LINGUEGLIA E, VOILLEY N, LAZDUNSKI M & BARBRY P. (1994). Biochemical analysis of the membrane topology of the amiloride- sensitive Na+ channel. *J Biol Chem* **269,** 12981-12986.

(6) CANESSA CM, MERILLAT AM & ROSSIER BC. (1994a). Membrane topology of the epithelial sodium channel in intact cells. *Am J Physiol Cell Physiol* **267,** C1682-C1690.

(7) SNYDER PM, MCDONALD FJ, STOKES JB & WELSH MJ. (1994). Membrane topology of the amiloride-sensitive epithelial sodium channel. *J Biol Chem* **269,** 24379-24383.

(8) ROSSIER BC, PRADERVAND S, SCHILD L & HUMMLER E. (2002). Epithelial sodium channel and the control of sodium balance: Interaction between genetic and environmental factors. *Annu Rev Physiol* **64,** 877-897

(9) FIRSOV D, GAUTSCHI I, MERILLAT AM, ROSSIER BC & SCHILD L. (1998). The heterotetrameric architecture of the epithelial sodium channel (ENaC). *EMBO J* **17,** 344-352.

(10) SNYDER PM, CHENG C, PRINCE LS, ROGERS JC & WELSH MJ. (1998). Electrophysiological and biochemical evidence that DEG/ENaC cation channels are composed of nine subunits. *J Biol Chem* **273,** 681-684.

(11) GARTY H & PALMER LG. (1997). Epithelial sodium channels: Function, structure, and regulation. *Physiol Rev* **77,** 359-396.

(12) FARMAN N, TALBOT CR, BOUCHER RC, FAY M, CANESSA C, ROSSIER B & BONVALET JP. (1997). Noncoordinated expression of alpha-, beta-, and gamma-subunit mRNAs of epithelial Na^+ channel along rat respiratory tract. *Am J Physiol* **272,** C131-141.

(13) HUMMLER E, BARKER P, GATZY J, BEERMANN F, VERDUMO C, SCHMIDT A, BOUCHER RC & ROSSIER BC. (1996). Early death due to defective neonatal lung liquid clearance in αENaC-deficient mice. *Nature Genet* **12,** 325-328.

(14) BARKER PM, NGUYEN MS, GATZY JT, GRUBB B, NORMAN H, HUMMLER E, ROSSIER B, BOUCHER RC & KOLLER B. (1998). Role of γ-ENaC subunit in lung liquid clearance and electrolyte balance in newborn mice. *J Clin Invest* **102,** 1634-1640.

(15) MCDONALD FJ, YANG B, HRSTKA RF, DRUMMOND HA, TARR DE, MCCRAY PB JR, STOKES JB, WELSH MJ & WILLIAMSON RA. (1999). Disruption of the beta subunit of the epithelial Na^+ channel in mice: hyperkalemia and neonatal death associated with a pseudohypoaldosteronism phenotype. *Proc Natl Acad Sci USA* **96,** 1727-1731.

(16) WALDMANN R, CHAMPIGNY G, BASSILANA F, VOILLEY N & LAZDUNSKI M. (1995). Molecular cloning and functional expression of a novel amiloride-sensitive Na+ channel. *J Biol Chem* **270,** 27411-27414.

(17) YAMAMURA H, UGAWA S, UEDA T, NAGAO M & SHIMADA S. (2004b). Protons activate the δ-Subunit of the epithelial Na^+ channel in humans. *J Biol Chem* **279,** 12529-12534.

(18) YAMAMURA H, UGAWA S, UEDA T, NAGAO M, JOH T & SHIMADA S. (2008a). Epithelial Na+ channel delta subunit is an acid sensor in the human oesophagus. *Eur J Pharmacol* **600,** 32-36.

(19) YAMAMURA H, UGAWA S, UEDA T, NAGAO M & SHIMADA S. (2008b). Epithelial Na+ channel delta subunit mediates acid-induced ATP release in the human skin. *Biochem Biophys Res Commun* **373,** 155-158.

(20) JI HL, SU XF, KEDAR S, LI J, BARBRY P, SMITH PR, MATALON S & BENOS DJ. (2006). Delta -subunit confers novel biophysical features to alpha beta gamma -human ENaC via a physical interaction. *J Biol Chem* **281,** 8233-8241.

(21) BANGEL-RULAND N, SOBCZAK K, CHRISTMANN T, KENTRUP D, LANGHORST H, KUSCHE-VIHROG KRISTINA & WEBER WM. (2009). Characterization of the epithelial sodium channel delta subunit in human nasal epithelium. *Am J Respir Cell Mol Biol* **42,** 498-505.

(22) YAMAMURA H, UGAWA S, UEDA T, NAGAO M & SHIMADA S. (2006). A novel spliced variant of the epithelial Na^+ channel δ-subunit in the human brain. *Biochem Biophys Res Commun* **349,** 317-321.

(23) JI HL & BENOS DJ. (2004). Degenerin sites mediate proton activation of δβγ-epithelial sodium channel. *J Biol Chem* **279,** 26939-26947.

(24) SU X, LI Q, SHRESTHA K, CORMET-BOYAKA E, CHEN L, SMITH PR, SORSCHER EJ, BENOS DJ, MATALON S, JI HL. (2006). Interregulation of proton-gated Na^+ channel 3 and cystic fibrosis transmembrane conductance regulator. *J Biol Chem* **281,** 36960-36968.

(25) ZHAO RZ, NIE HG, SU XF, HAN DY, LEE A, HUANG Y, CHANG Y, MATALON S & JI HL. (2012). Characterization of a novel splice variant of δ ENaC subunit in human lungs. *Am J Physiol Lung Cell Mol Physiol* **302,** L1262-L1272.

(26) BURRI PH. (1997). Structural aspects of prenatal and postnatal development and growth of the lung. In: MCDONALD JA (Ed.), *Lung Growth and development*, vol 100. Marcel Dekker, New York, 1-35.

(27) HELMS MN, SELF J, BAO HF, JOB LC, JAIN L, EATON DC. (2006). Dopamine activates amiloride-sensitive sodium channels in alveolar type I cells in lung slice preparations. *Am J Physiol Lung Cell Mol Physiol* **291,** L610-L618.

(28) JOHNSON MD, BAO HF, HELMS MN, CHEN XJ, TIGUE Z, JAIN L, DOBBS LG & EATON DC. (2006). Functional ion channels in pulmonary alveolar type I cells support a role for type I cells in lung ion transport. *Proc Natl Acad Sci USA* **103,** 4964-4969.

(29) DOBBS LG & JOHNSON MD. (2007). Alveolar epithelial transport in the adult lung. *Respir Physiol Neurobiol* **159,** 283-300.

(30) QIAO R, ZHOU B, LIEBLER JM, LI X, CRANDALL ED & BOROK Z. (2003). Identification of three genes of known function expressed by alveolar epithelial type I cells. *Am J Respir Cell Mol Biol* **29,** 98-105.

(31) DAHLIN K, MAGER EM, ALLEN L, TIGUE Z, GOODGLICK L, WADEHRA M & DOBBS L. (2004). Identification of genes differentially expressed in rat alveolar type I cells. *Am J Respir Cell Mol Biol* **31,** 309-316.

(32) WRIGHT JR & HAWGOOD S. (1989). Pulmonary surfactant metabolism. *Clin Chest Med* **10,** 83-93.

(33) KIM KK, KUGLER MC, WOLTER PJ, ROBILLARD L, GALVEZ MG, BRUMWELL AN, SHEPPARD D & CHAPMAN HA. (2006). Alveolar epithelial cell mesenchymal transition develops in vivo during pulmonary fibrosis and is regulated by the extracellular matrix. *Proc Natl Acad Sci U.S.A.* **103,** 13180-13185.

(34) OLVER RE & STRANG LB. (1974). Ion fluxes across the pulmonary epithelium and the secretion of lung liquid in the foetal lamb. *J Physiol* **241,** 327-357.

(35) MATTHAY MA, FOLKESSON HG & VERKMAN AS. (1996). Salt and water transport across alveolar and distal airway epithelia in the adult lung. *Am J Physiol* **270,** L487-L503.

(36) EATON DC, HELMS MN, KOVAL M, BAO HF & JAIN L. (2008). The contribution of epithelial sodium channels to alveolar function in health and disease. *Annu Rev Physiol* **71,** 403-423.

(37) JAIN L, CHEN XJ, RAMOSEVAC S, BROWN LA, EATON DC. (2001). Expression of highly selective sodium channels in alveolar type II cells is determined by culture conditions. *AM J Physiol Lung Cell Mol Physiol* **280,** L646-658.

(38) CHEN XJ, EATON DC & JAIN L. (2002). β-Adrenergic regulation of amiloride-sensitive lung sodium channels. *Am J Physiol Lung Cell Mol Physiol* **282,** 609-620.

(39) JAIN L, CHEN XJ, BROWN LA, EATON DC. (1998). Nitric oxide inhibits lung sodium transport through a cGMP-mediated inhibition of epithelial cation channels. *Am J Physiol* **274,** L475-L484

(40) HELMS MN, JAIN L, SELF JL, EATON DC. (2008). Redox regulation of epithelial sedum channels (ENaC) examined in alveolar type 1 and 2 cell patch clamped in lung slice tissue. *J Biol Chem* **283,** 22875-22883.

(41) EATON DC & JAIN L. (2006). Ion channels: an overview. In: Shapiro SD (Ed) & Laurent GJ, *Encyclopedia of Respiratory Medicine.* Oxford, UK: Elsevier **1,** 1-4

(42) MATALON S, LAZRAK A, JAIN L & EATON DC. (2002). Lung edema clearance: 20 years of progress. Invited review: biophysical properties of sodium channels in lung alveolar epithelial cells. *J Appl Physiol* **93,** 1852-1859.

(43) JUNOR RW, BENJAMIN AR, ALEXANDROU D, GUGGINO SE & WALTERS DV. (1999). A novel role for cyclic nucleotide-gated cation channels in lung liquid homeostasis in sheep. *J Physiol* **520 (Pt 1),** 255-260.

(44) LI T & FOLKESSON HG. (2006). RNA interference for α-ENaC inhibits rat lung fluid absorption in vivo. *Am J Physiol Lung Cell Mol Physiol* **290,** L649-660.

(45) HAMILTON KL & EATON DC. (1985). Single-channel recordings from amiloride-sensitive epithelial sodium channel. *Am J Physiol Cell Physiol* **249,** C200-C207.

(46) HAMER PW, MCGEACHIE JM, DAVIES MJ & GROUNDS MD. (2002). Evans Blue Dye as an *in vivo* marker of myofibre damage: optimising parameters for detecting initial myofibre membrane permeability. *J Anat* **200,** 69–79.

(47) YAMAMURA H, UGAWA S, UEDA T & SHIMADA S. (2005a). Evans blue is a specific antagonist of the human epithelial Na^+-channel delta-subunit. *J Pharmacol Exp Ther* **315,** 965-969.

(48) BEVAN S, HOTHI S, HUGHES G, JAMES IF, RANG HP, SHAH K, WALPOLE CSJ & YEATS JC. (1992). Capsazepine: a competitive antagonist of the sensory neurone excitant capsaicin*. Br J Pharmacol* **107,**544–552.

(49) SZALLASI A, GOSO C, BLUMBERG PM & MANZINI S. (1993). Competitive inhibition by capsazepine of [3H]resiniferatoxin binding to central (spinal cord and dorsal root ganglia) and peripheral (urinary bladder and airways) vanilloid (capsaicin) receptors in the rat. *J Pharmacol Exp Ther* **267,** 728-733.

(50) SZALLASI A & BLUMBERG PM. (1999). Vanilloid (Capsaicin) Receptors and Mechanisms. *Pharmacol Rev* **51,** 159-212.

(51) KUENZI FM & DALE N. (1996). Effect of capsaicin and analouges on potassium and calcium currents and vanilloid receptors in Xenopus embryo spinal neurones. *British Journal of Pharmacology* **119,** 81-90.

(52) DOCHERTY RJ, YEATS JC & PIPER AS. (1997). Capsazepine block of voltage-activated calcium channels in adult rat dorsal root ganglion neurones in culture. *Br J Pharmacol* **121,** 1461-1467.

(53) LIU L & SIMON SA. (1997). Capsazepine, a vanilloid receptor antagonist, inhibits nicotinic acetylcholine receptors in rat trigeminal ganglia. *Neuroscience Letters* **228,** 29-32.

(54) YAMAMURA H, UGAWA S, UEDA T, NAGAO M & SHIMADA S. (2004a). Capsazepine is a novel activator of the delta subunit of the human epithelial Na^+-channel. *J Biol Chem* **279,** 44483-44489.

(55) MCKEMY DD, NEUHAUSSER WM & JULIUS D. (2002). Identification of a cold receptor reveals a general role for TRP channels in thermosensation. *Nature* **416,** 52-58.

(56) STORY GM, PEIER AM, REEVE AJ, EID SR, MOSBACHER J, HRICIK TR, EARLEY TJ, HERGARDEN AC, ANDERSSON DA, HWANG SW, MCINTYRE P, JEGLA T, BEVAN S & PATAPOUTIAN A. (2003). ANKTM1, a TRP-like channel expressed in nociceptive neurons, is activated by cold temperatures. *Cell* **112,** 819-829.

(57) ANDERSSON DA, CHASE HW & BEVAN S. (2004). TRPM8 activation by menthol, icilin and cold is differentially modulated by intracellular pH. *J Neurosci* **24,** 5364-5369.

(58) YAMAMURA H, UGAWA S, UEDA T, NAGAO M & SHIMADA S. (2005b). Icilin activates the delta-subunit of the human epithelial Na^+ channel. *Mol Pharmacol* **68,** 1142-1147.

(59) WESCH D, ALTHAUS M, MIRANDA P, CRUZ-MUROS I, FRONIUS M, GONZALEZ-HERNANDEZ T, CLAUSS WG, ALVAREZ DE LA ROSA D & GIRALDEZ T. (2011). Differential N termini in epithelial Na^+ channel δ-subunit isoforms modulate channel trafficking to the membrane. *Am J Physiol Cell Physiol* **302,** C868-879.

(60) HOLLYWOOD MA, COTTON KD, MCHALE NG & THORNBURY KD. (1998). Enhancement of Ca^{2+}-dependent outward current in sheep bladder myocytes by evans blue dye. *Pflueg Arch Eur J Physiol* **435,** 631-636.

(61) WU SN, JAN CR, LI HF & CHEN SA. (1999). Stimulation of large-conductance Ca^{2+}-activated K^+ channels by Evans blue in cultured endothelial cells of human umbilical veins*. Biochem Biophys Res Commun* **254,** 666-674.

(62) CHUANG HH, NEUHAUSSER WM & JULIUS D. (2004). The super-cooling agent icilin reveals a mechanism of coincidence detection by temperature-sensitive TRP channel. *Neuron* **43,** 859-869.

LEBENSLAUF

NAME: SVENJA SLADEK
ADRESSE: UFERSTRASSE 3, D-94557 NIEDERALTEICH
TELEFONNUMMER: 0049/176/24790311

PERSÖNLICHE INFORMATION

GEBURTSDATUM: 01.06.1985
GEBURTSORT: NEUENDETTELSAU
NATIONALITÄT: DEUTSCH
FAMILIENSTAND: LEDIG

AUSBILDUNG

SEIT WS 20006/07	STUDIUM DER PHARMAZIE, UNIVERSITÄT WIEN
WS 2004/05 – SS 2006	EUROPEAN ECONOMIC STUDIES, OTTO-FRIEDRICH-UNIVERSITÄT BAMBERG
1995 - 2004	ST. GOTTHARD GYMNASIUM, NIEDERALTEICH ABITUR IN ENGLISCH/MUSIK
1991 - 1995	ABT-JOSCIO-GRUNDSCHULE, NIEDERALTEICH

BERUFSERFAHRUNG

SEIT MAI 2009	MITARBEITERIN DER GERMANIA APOTHEKE, WIEN
SEPTEMBER 2008	PRAKTIKUM IN DER KRANKENHAUSAPOTHEKE, KLINIKUM DEGGENDORF
SEPT – OKT 2007	KOPIERSTUDENTIN BEI OCTAPHARMA, WIEN BEREICH: MEDIKAMENTENZULASSUNG

SPRACHEN

ENGLISCH	FLIESSEND IN WORT UND SCHRIFT
SPANISCH	GUTE KENNTNISSE
LATEIN	ABSCHLUSS DES KLEINEN LATINUMS

WEITERE QUALIFIKATIONEN

EDV-KENNTNISSE: MS-OFFICE - WORD, POWER POINT,
EXCEL, APOTHEKENBETRIEBSSYSTEM DATAPHARM